Journal of Medicinal Chemistry

pubs.acs.org/jmc

Article

Design, Synthesis, and Activity Evaluation of Stereoconfigured Tartarate Derivatives as Potential Anti-inflammatory Agents *In Vitro* and *In Vivo*

Priya Kumari, Palwinder Singh,* Jashanpreet Kaur, and Rajbir Bhatti

Cite This: *J. Med. Chem.* 2021, 64, 9550−9566

Read Online

ACCESS | Metrics & More | Article Recommendations | Supporting Information

ABSTRACT: Preclinical and clinical data reveal that inflammation is strongly correlated with the pathogenesis of a number of diseases including those of cancer, Alzheimer, and diabetes. The inflammatory cascade involves a multitude of cytokines ending ultimately with the activation of COX-2/LOX for the production of prostaglandins and leukotrienes. While the available inhibitors for these enzymes suffer from nonoptimal selectivity, in particular for COX-2, we present here the results of purposely designed tartarate derivatives that exhibit favorable selectivity and significant effectiveness against COX-2 and LOX. Integrated approaches of molecular simulation, organic synthesis, and biochemical/physical experiments identified **15** inhibiting COX-2 and LOX with respective IC_{50} 4 and 7 nM. At a dose of 5 mg kg^{-1} to Swiss albino mice, **15** reversed algesia by 65% and inflammation by 33% in 2−3 h. We find good agreement between experiments and simulations and use the simulations to rationalize our observations.

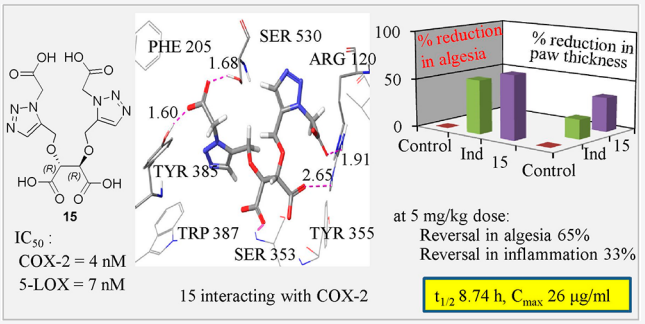

INTRODUCTION

Inflammation is the body's first alarm signal in response to microbial invaders and pathogens whereas its continuing prevalence (chronic) can lead to the development of several diseases such as cardiovascular disease, cancer, Alzheimer's disease, asthma, rheumatoid arthritis, and diabetes.[1−6] Succeeding the discovery of cyclooxygenase[7] and its two isoforms COX-1 and COX-2,[8−10] the cascade of arachidonic acid (AA) metabolism is extensively explored identifying PGE_2, PGD_2, PGF_2, and LT_4s′ (Figure 1) as the causative agents of inflammation. Though LX_4 has been reported to have an anti-inflammatory effect,[11,12] the pronounced inflammatory consequences of LTB_4, LTC_4, LTD_4, and LTE_4 make LOX an attractive target for inflammation therapy. These metabolites are generated by the inducible COX-2 and LOX under cell signaling initiation by the activation of inflammatory cytokines.[10] It is also thought that similar to the previous corona viruses, such as SARS-CoV,[16] the deaths induced by SARS-CoV-2 (COVID-19) are due to the systemic inflammation caused by "cytokine storms" propelled by pro-inflammatory cytokines including tumor necrosis factor-α (TNF-α), interleukin-1/6 (IL-1/6), and interferon-γ (INF-γ). One such small but potent signaling protein, IL-6, is a call-to-arms for the macrophages which besides fueling inflammation also damages normal cells. The ideal counter, then, would be the drugs that block the activity of COX-2 and LOX- reducing the formation of PGE_2, PGD_2, PGF_2, and the leukotrienes (enclosed in red boxes in Figure 1).

While a number of steroidal and nonsteroidal drugs regulating a broad range of inflammatory diseases by targeting COX-2 are identified, the parallel existence of house-keeping COX-1[17] led to the emergence of selective COX-2 inhibitors (COXIBS).[18−21] However, the cardiovascular side effects of these COX-2 inhibitory drugs were responsible for the withdrawal of rofecoxib and valdecoxib[22,23] leaving only celecoxib[24,25] for the treatment of arthritis, acute pain, and menstrual pain. Since the blockage of the COX-2 channel during the use of COXIBS shifts the AA gradient to the lipoxygenase and COX-1 channels,[26] resulting in the higher production of leukotrienes, the advantage of targeting both LOX and COX-2[27−29] motivated us to develop dual COX-2/LOX inhibitors. As of now, besides the medicinal use of celecoxib[24,25] and zileuton,[30] though these are also associated with side effects,[31−35] not many dual COX-2/LOX inhibitors[29,36−42] are succeeded to the clinical trials/practice (Figure 2).

Although the heterocycles-templated biaryl substituted classical COX-2 inhibitors such as celecoxib (Figure 3A)[20,43] are found to occupy the AA binding pocket of COX-2,[26] it

Received: May 16, 2021
Published: June 17, 2021

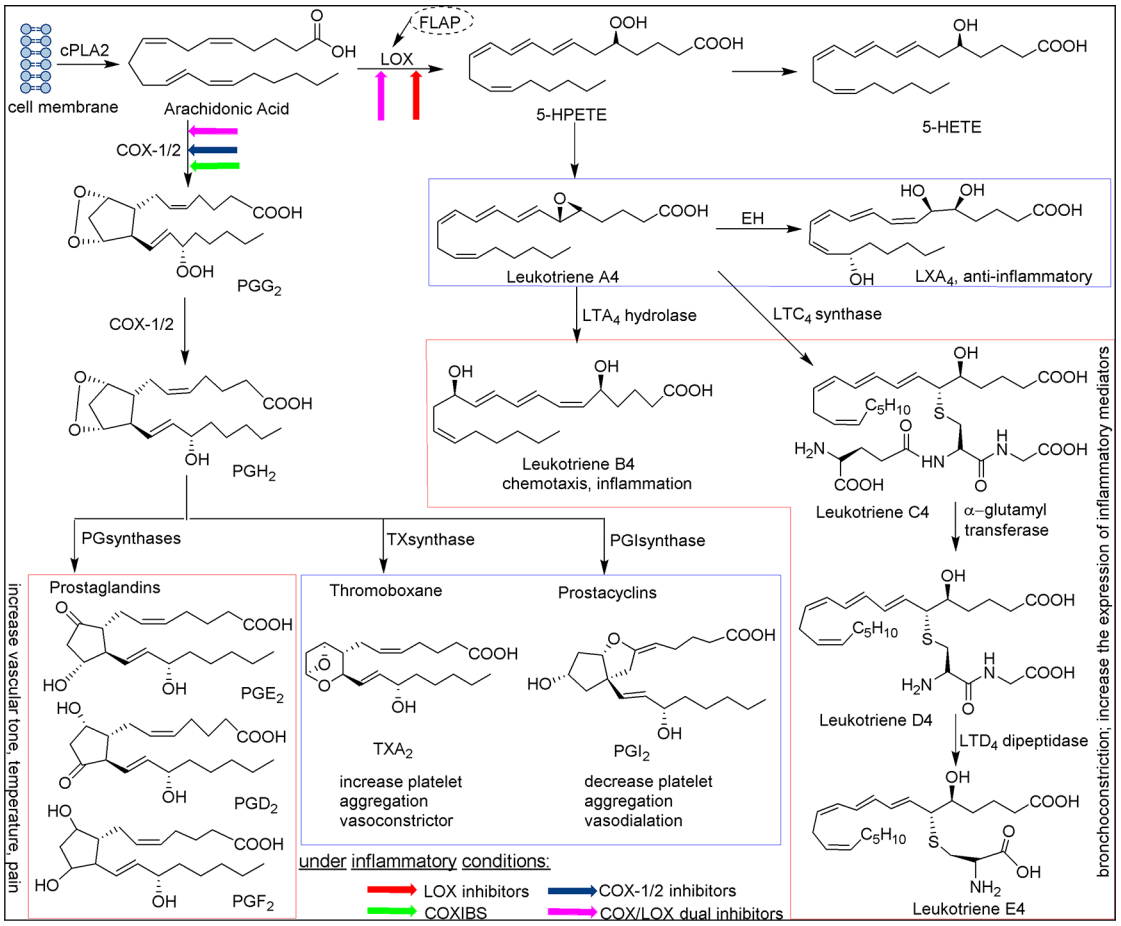

Figure 1. AA metabolism cascade.[13−15] Inflammatory house-keeping prostaglandins/leukotrienes are respectively enclosed in red and blue boxes. Colored arrows indicate COX-2/LOX targeting.

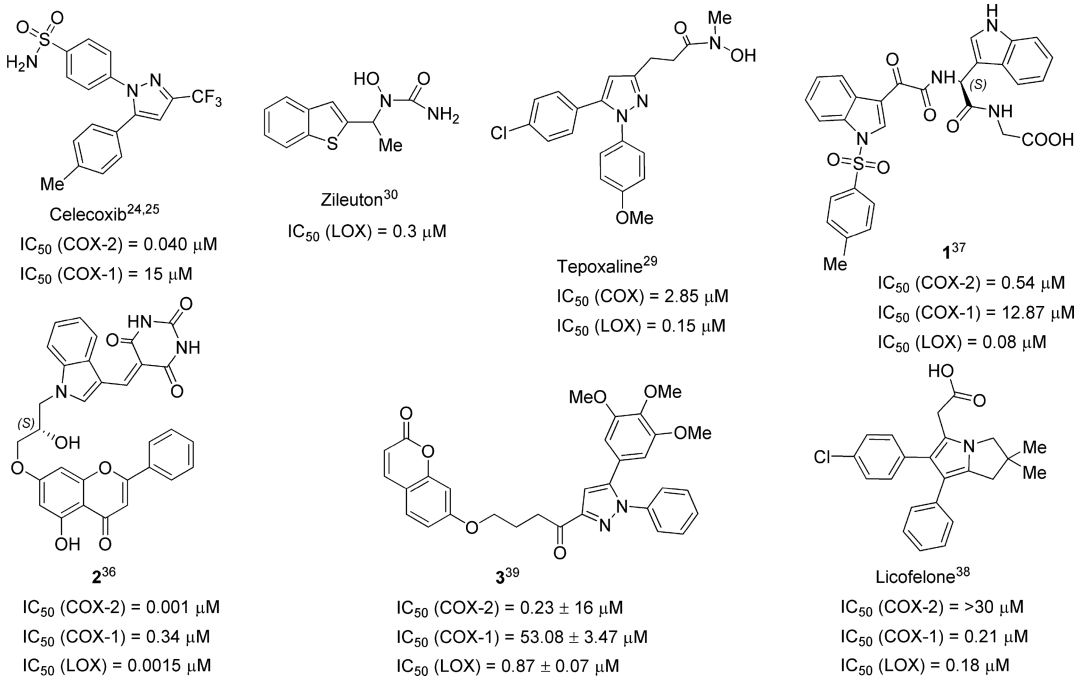

Figure 2. COX-2, 5-LOX, and COX-2/5-LOX dual inhibitors. **1**−**3** refer to numbering in the original publication.

would appear that it is relatively rare to have tartarate based acyclic-templated COX-2/LOX inhibitors which can attain a conformation similar to that of AA (Figure 3B) and hence can better occupy the active site pocket of the enzymes. Thence,

https://doi.org/10.1021/acs.jmedchem.1c00880
J. Med. Chem. 2021, 64, 9550−9566

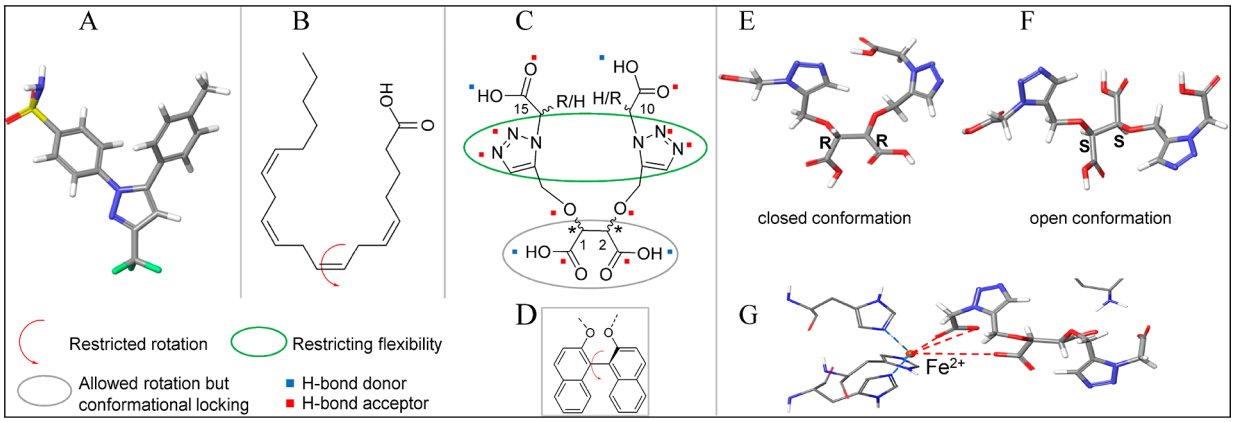

Figure 3. Overall design strategy for new COX-2, LOX inhibitors. (A) Energy minimized geometry of celecoxib. (B) U-shaped conformation of arachidonic acid as attained in the active site pocket of the enzymes. (C) New molecules with conformation similar to that of AA showing H-donor/acceptor sites. (D) Binol moiety. Energy minimized conformation of (E) (1*R*,2*R*)-**15** and (F) (1*S*,2*S*)-**15**. (G) Interactions of **15** with Fe^{2+} of 5-LOX (from molecular docking studies).

Scheme 1. Synthesis of Key Intermediates 4 and 5[a]

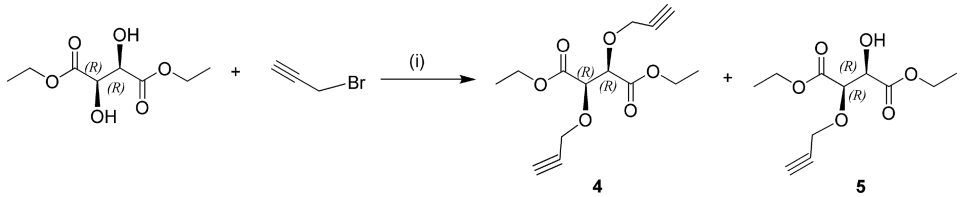

[a]Reaction conditions: (i) NaH, THF, 18-crown-6, tetrabutylammonium bromide, 0−25 °C.

for creating inhibitors structurally similar to AA, tartarate was chosen as one of the components of new molecules. The biological acceptance, capability to undergo polar/nonpolar interactions with the protein, and providing another asymmetric carbon/s (except glycine) led us to choose amino acids for coupling with tartarate. Making use of amino acid azides, while creating an additional medicinally functional unit 1,2,3-triazole,[44,45] the desired bending (so to achieve AA like structure) in the substituent chains may be achieved (Figure 3C). It was, therefore, envisaged that the appropriate stereochemistry at the two asymmetric carbons of tartarate and its sufficient backbone flexibility may confer L-/extended-U shaped geometry to the molecule enabling it to go over the AA binding pocket of the enzyme. As a proof of concept, an energy minimized closed conformation was observed for the (1*R*,2*R*)-tartarate based molecules (Figure 3E) whereas their (1*S*,2*S*)-isomer attained an open conformation (Figure 3F). A pertinent role of the flexible hydrophilic tartarate moiety was warranted by replacing it with rigid hydrophobic binol (Figure 3D). The designed molecules were also intended to orchestrate Fe^{2+}/Fe^{3+} of LOX as observed in the molecular docking studies (Figure 3G). Based on this design, molecules **6**−**23** (Figure S1, Schemes 1−5) were synthesized and evaluated for in vitro COX-2/COX-1/LOX inhibitory activity using enzyme immunoassays, examined for the in vivo suppression of analgesia and inflammation, and checked for acute toxicity, mode of action, pharmacokinetics, and interactions with the enzymes as detailed below.

The molecular simulations with the stereoisomers of **6**−**23** were performed to make an initial assessment of their bioactive conformations by evaluating the differences of their (stereoisomers) interactions in the active sites of COX-2 and 5-LOX. It was observed that in comparison to the stereoisomers with 1*S*,2*S* and 1*S*/1*R*, 2*R*/2*S* configurations at the two carbons of tartarate, the isomers with 1*R*, 2*R* stereochemistry exhibit better interactions with 5-LOX (PDB ID 3V99) (5-LOX was chosen because all the compounds dock in this enzyme) (Table S1). Moreover, in addition to the 1*R*,2*R* stereochemistry, the isomers with either both 10*S*, 15*S* or 10*S*/10*R*, 15*R*/15*S* (Figure 3C for numbering) were better interacting with the enzyme. Out of the 10 stereoisomers 8a, 8b/8c, 8d, 8e, 8f/8n, 8g/8h, 8i, 8j/8k, 8l/8m, and 8o of compound **8** (the pairs 8b/8c, 8f/8n, 8g/8h, 8j/8k, and 8l/8m were the same), 8a and 8g/8h with respective configurations 1*R*, 2*R*, 10*S*, 15*S*, and 1*R*, 2*R*, 10*S*/10*R*, 15*R*/15*S* exhibited maximum interactions with the active site residues of 5-LOX (Table S1). The docking score of 8a and 8g/h was also significantly better than the other isomers. Similar results were obtained when the stereoisomers of the rest of the compounds were docked in the active sites of COX-2 and 5-LOX (Table S2, S3). As a result, instead of synthesizing all isomers of the designed compounds, we restricted to those with 1*R*, 2*R*, 10*S*, 15*S* configurations. Only in the case of compound **8**, the isomer **8g/h** with 1*R*, 2*R*, 10*S*/10*R*, 15*R*/15*S* configuration was synthesized for the purpose of comparison. Some other implications of the molecular docking studies including poor interactions of binol derivatives in the active site pocket of COX-2 and better interactions of the carboxylate compounds than their ester analogues were also supported by the results of enzyme immunoassays.

RESULTS AND DISCUSSION

Chemistry. The syntheses of the designed molecules are depicted in Schemes 1−5. Reaction of (1*R*,2*R*)-diethyl tartarate with propargyl bromide provided key intermediates

https://doi.org/10.1021/acs.jmedchem.1c00880
J. Med. Chem. 2021, 64, 9550−9566

Scheme 2. Synthesis of Compounds 6−10[a]

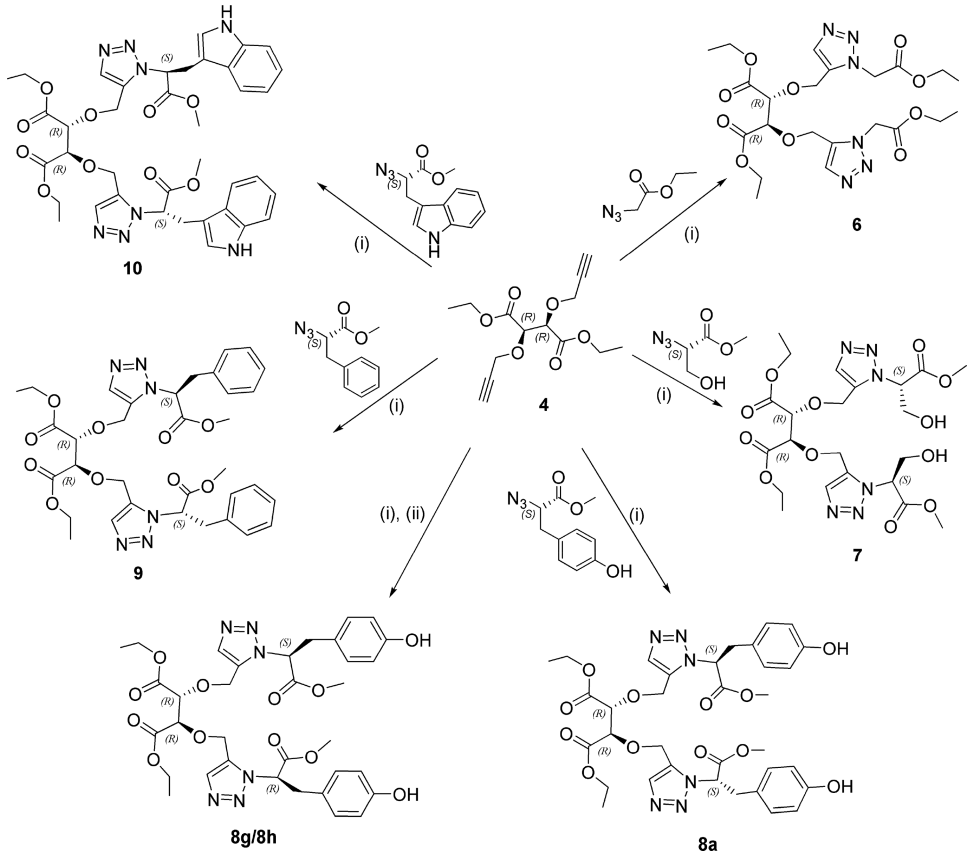

[a](i) EtOH:water (9:1), sodium ascorbate, $CuSO_4.5H_2O$, room temperature. For **8g/h**: (i) (*S*)-tyrosine azide (1 equiv), (ii) (*R*)-tyrosine azide (1 equiv).

Scheme 3. Synthesis of Compounds 11−14[a]

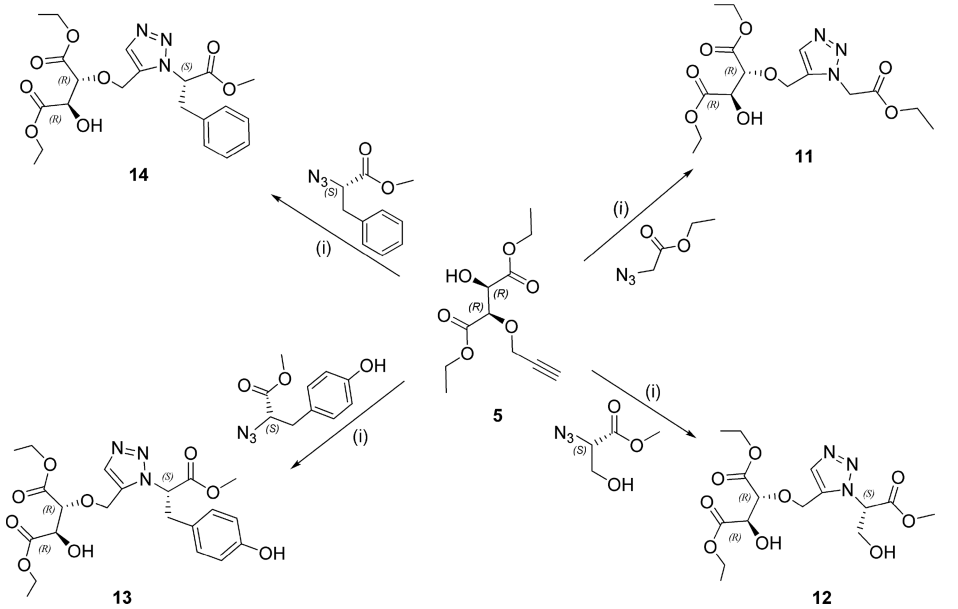

[a](i) EtOH:water (9:1), sodium ascorbate, $CuSO_4.5H_2O$, room temperature.

4 (40%) and **5** (15%) (Scheme 1). For incorporating the amino acid derived 1,2,3-triazole moiety in the molecule, intermediate **4** was coupled with ethylbromoacetate azide/(*S*)-serine azide/(*S*)-tyrosine azide/(*S*)-phenylalanine azide/(*S*)-tryptophenyl azide at room temperature in the presence of sodium ascorbate and copper sulfate, and compounds **6−10** were generated (Scheme 2). In a two step procedure, treatment of **4** with (*S*)-tyrosine azide (1 equiv) and further

https://doi.org/10.1021/acs.jmedchem.1c00880
J. Med. Chem. 2021, 64, 9550−9566

reaction of monosubstituted product with another equivalent of (*R*)-tyrosine azide gave compound **8g/h**. Compound **8g/h** exhibited the same spectral data as compound **8a** except a difference in the optical rotation. Similar to the reactions of **4** with the azides, intermediate **5** was also made to react with ethylbromoacetate azide, (*S*)-serine azide, (*S*)-tyrosine azide, and (*S*)-phenylalanine azide to procure compounds **11**−**14** (Scheme 3). In order to make comparison of the biological activities, the ester moieties of **6** and **9** were transformed to their corresponding acids in compounds **15** and **16**, respectively (Scheme 4).

Scheme 4. Synthesis of Compounds 15 and 16[a]

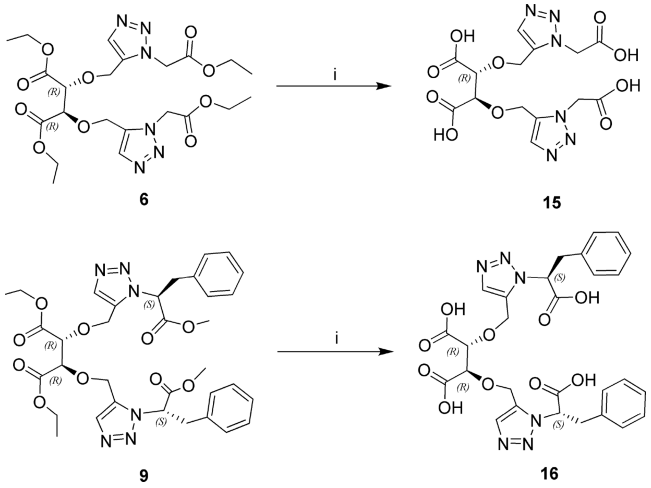

[a](i) Acetone:water (3:2), NaOH, room temperature.

Further, as it was envisaged that the acyclic tartarate moiety may be better suited to provide an AA like structure to the molecules, the hypothesis was checked by replacing it with binol. The reactions of compound **18**, obtained by the propargylation of (*S*)-binol (**17**), with the same azides as used in Schemes 2 and 3 gave products **19**−**23** (Scheme 5). All the synthesized compounds were characterized by using NMR, IR, and HRMS techniques (Experimental Section, SI).

Biological Studies. *In Vitro COX-1/2 and LOX Inhibitory Assay.* By performing enzyme immunoassays,[46,47] the activities of compounds **6**−**16** and **19**−**23** against COX-1/2 and LOX were determined at 10^{-4}−10^{-8} M concentrations in triplicate. These were calculated by measuring the amount of prostaglandins/leukotrienes produced in each enzymatic reaction and quantified in terms of 50% inhibitory concentrations (IC_{50}). Compounds **6** and **8a**, **8g**/**8h** exhibited significant inhibitory activity for COX-2 with respective IC_{50} values 0.1 and 0.7 μM, but their selectivity for COX-2 over COX-1 was either too high (600) or too low (∼14). Although the IC_{50} of compound **7** was 0.4 μM, its selectivity for COX-2 over COX-1 was found between that of celecoxib (COX-2 selective) and indomethacin (COX-1/2 nonselective). Compound **10** exhibited the IC_{50} value 0.5 μM for COX-2. Besides their poor interactions with COX-2, the binol compounds were included in the enzyme immunoassays so that the results of molecular modeling studies get validated. It was noticed that the replacement of the tartarate fragment of compounds **6**−**10** with the binol in compounds **19**−**23** lowered the potency of the compounds against both COX-2 and LOX (Table 1). Compounds **11**−**14** with substitution at only one OH group of tartarate displayed lower potency than that of compounds **6**−**10**. While identifying a new inhibitor, it was observed that compound **15** exhibited dramatically better COX-2 and LOX inhibitory activity than all the other compounds including the positive controls celecoxib and zileuton. Desirably, the selectivity index 75 of compound **15** also fell between that of selective (celecoxib) and nonselective (indomethacin) COX-2 inhibitors. In general, compounds **8**, **9**, and **10** with an aromatic side chain at C_α of the amino acid component of the molecule exhibited lower potency for COX-2 but better for LOX suggesting that the binding interface of LOX can accommodate relatively bulky and lipophilic groups. This trend in the inhibitory activity of the compounds is similar to the results of molecular docking studies where the aromatic moiety of the amino acid did not allow the molecule to fit into the active site of COX-2. Moreover, supporting the in-silico results, compound **8g/h** was found as potent as its stereoisomer **8a**. On the basis of the structure activity relationship studies, it was inferred that either no or a small side chain at C_α of the amino acid unit of these molecules seems to be optimal for the COX-2 inhibitory activity. Overall, compounds **6**, **7**, **8a**, **10**, **15**, **16**, and **21** were identified for further screening on animal models.

Human Whole Blood Assay.[46,48] Human whole blood assay was performed to support the results of enzyme immunoassays for the selectivity of compound **15** for COX-2 over COX-1. Here, the lipopolysaccharide (LPS) induced expression of COX-2 was reversed (Figure 4A) whereas no effect on calcium ionophore induced expression of COX-1 was observed (Figure 4B) (Table 2).

In Vivo Screening of the Compounds. The anti-inflammatory and analgesic activities of the compounds were checked on Swiss albino mice (25−35 g) of either sex.

Acetic Acid-Induced Writhing Test. Stretching of abdomen and extension of hind-limbs[49] were specified in acetic acid-induced writhing test for evaluating the analgesic activities of the compounds. The standard and the test groups of animals were given indomethacin (10 mg kg^{-1}) and test compounds (5 mg kg^{-1}), respectively, 30 min before inducing the writhings through 0.6% v/v acetic acid injection (including the control group). The results recorded in terms of reduction in the number of writhings are shown in Figure 5A. Compound **15** treated animals caused 65% inhibition of algesia that was appreciably better than the 55% shown by the standard drug indomethacin and comparable to the 62% analgesic effect of celecoxib at 5 mg kg^{-1} dose.[50] The analgesic activity of **6** and **7** was almost in parallel to their response in enzyme immunoassays whereas other compounds included in these experiments were not very effective in reducing the number of writhings.

Carrageenan Induced-Paw Edema Test. It is an acute inflammatory model[51] in which the reduction in carrageenan-induced thickness of hind paw in the presence of the test compounds was taken as a measure of their anti-inflammatory activity. The control, standard, and treatment groups of animals were given indomethacin (10 mg kg^{-1}) and the test compounds (5 mg kg^{-1}), respectively, 30 min prior to the 100 μL injection of freshly prepared 1% carrageenan solution. The paw thickness (mm) was determined at 15, 30, 60, 120, 180, 240, 300, and 360 min time intervals. It was apparent from Figure 5B that compound **15** (5 mg kg^{-1}) caused a 33% decrease in the paw edema that was significantly better than the 30% decrease caused by indomethacin at 10 mg kg^{-1} and comparable to the 33% reduction shown by celecoxib at 5 mg

https://doi.org/10.1021/acs.jmedchem.1c00880
J. Med. Chem. 2021, 64, 9550−9566

Scheme 5. Synthesis of Compounds 19−23[a]

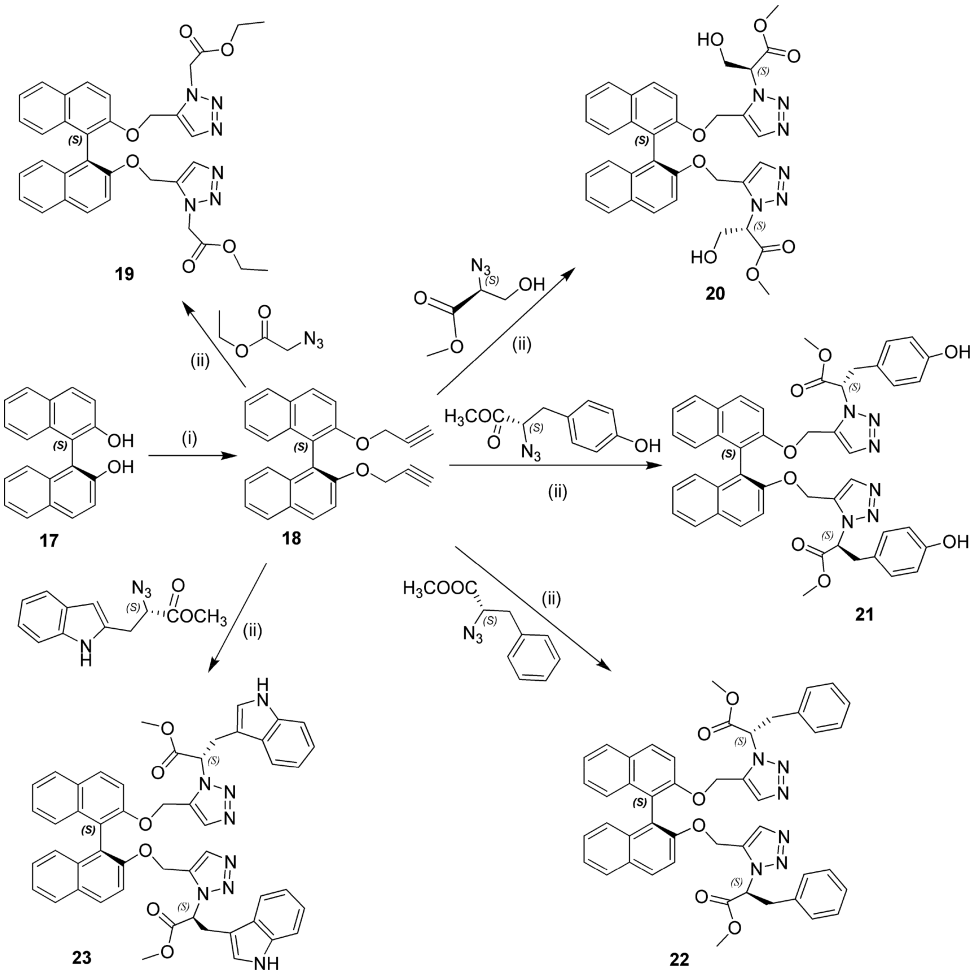

[a](i) Acetone, anhydrous potassium carbonate, propargyl bromide, 60 °C, (ii) EtOH:water (9:1), sodium ascorbate, $CuSO_4.5H_2O$, room temperature.

kg^{-1} dose.[50] Moreover, the anti-inflammatory effect of compound **15** was observed after 2−3 h (Figure 5C) of treatment against the similar effect of indomethacin and celecoxib in 5−6 h and 3−4 h,[50] respectively. This observation points toward the fast-acting feature of **15** (Figure S109) though more experiments are needed to prove it. The response of compound **21**, kept for positive comparison, was similar to its poor analgesic effect.

Further, to check the dose-dependent anti-inflammatory effect of compound **15**; its 0.5, 2.5, 5, 10, and 20 mg kg^{-1} doses were given to 5 sets of animals (6 animals in each group) 30 min prior to carrageenan injection, and percentage decrease in paw thickness (mm) was determined (Figure 5C, Table 3). Characteristically, a dose-dependent response in terms of decrease in paw thickness was observed and the effect achieved saturation between 5 and 10 mg kg^{-1} dose (Figure 5D).

Mechanistic Study. In addition to the enzyme immunoassay, in vivo studies were also performed to check if these compounds target COX-2/LOX pathways. Substance P (10 μg kg^{-1}) was used to study the involvement of COX-2 and LOX pathways whereas the nitric oxide donor L-arginine (40 mg kg^{-1}) and the nitric oxide synthase inhibitor N6-(1-iminoethyl)-L-lysine dihydrochloride (L-NIL) (5 mg kg^{-1}) were utilized to study the participation of the nitric oxide pathway. All these prescriptions were given intraperitoneally 30 min before the treatment with compound **15**. After 30 min, each group of animals was treated with 0.6% v/v acetic acid, and the number of abdominal writhings was noted for 30 min. Pretreatment with Substance P (COX-2 and LOX stimulator) made a significant reversal in the effect of compound **15**, delineating that **15** might induce its analgesic effect by inhibiting COX-2 and LOX pathways. L-arginine (nitric oxide donor) treatment did not change the analgesic effect of **15**. However, pretreatment with L-NIL, a nitric oxide synthase inhibitor, potentiated the effect of compound **15** (Figure 6). Hence, the results of these in vivo experiments suggested nonimplication of the NO pathway in modulating the analgesic effect of compound **15**.

Acute Toxicity Study. Acute toxicity studies were carried out using Swiss albino mice. Briefly, 2 groups were used with three animals in each group (n = 3). The first group was normal control whereas in the second group, compound **15** was given orally a dose of 300 mg kg^{-1} (due to quite low IC_{50} value, only 300 mg kg^{-1} dose was used for toxicity studies). The study was performed after 4 h of the fasting period. Mice were continuously monitored for a period of 4 h followed by periodic monitoring for the next 14 days. Mice exhibited a sedative effect after 1 h of the treatment with slowed movements, sluggish behavior, and sleep. The effects subsided within the next 1 h. No other gross behavioral changes were

https://doi.org/10.1021/acs.jmedchem.1c00880
J. Med. Chem. 2021, 64, 9550−9566

Table 1. IC_{50} (μM) Values of Compounds 6−23 against COX-1, COX-2, and LOX

Compounds	IC_{50} (μM)[a] COX-1	COX-2	LOX	Selectivity index[b]
6	60	0.1	0.3	600
7	54	0.4	1.3	135
8a	>10	0.7	0.15	>14
8g/h	>10	0.7	0.14	>14
9	90		0.09	
10	>10	0.5	0.45	>20
11	95	55	6	1.7
12	110	40	14	2.7
13	80	35	12	2.3
14	55	32	8	1.7
15	0.3	0.004	0.007	75
16	1.0	1.0	0.5	1
19	70	23	11	3.0
20	86	30	6	2.8
21	>10	1.5	0.6	>7
22	150	54	3	2.7
23	90	2.8	1.0	32
Indomethacin	0.08	0.96		0.08
Diclofenac	0.07	0.02		3.5
Celecoxib	15	0.04		375
Zileuton			0.3	

[a]Average of three values with deviation <3%. [b]IC_{50} (COX-1)/(COX-2).

observed. Due to the ethical issues, the animals were not sacrificed, and hence the images of the organs were not taken. The toxicities of compounds **6**, **8**, **10**, and **15**, alone as well as in combination with LPS, were also checked over the microglial cells BV2. Though the results are not shown here, all these compounds exhibited no toxicity to the cells (checked up to 48 h) even at concentration >1 μM.

Pharmacokinetics of ***15***. A dose of 10 mg kg^{-1} of 0.1% CMC suspension of **15** was administered i.p. to the Swiss albino mice. This compound exhibited $t_{1/2}$ of 8.74 h and attained a maximum concentration (C_{max}) of 26 μg/mL in 1 h of its administering to the animal (Figure 7, Table 4). Even after 24 h, the plasma drug concentration (1.98 μM) was above the IC_{50} required for COX-2/LOX inhibition as determined in the enzyme assays. The Cl value 0.0355 (μg/mL)/h indicates that it takes ∼35h for the complete clearance of the compound

Table 2. Inhibition of TXB_2 during Calcium Ionophore Stimulation and PGE_2 in LPS Stimulation of Human Whole Blood by Compound 15

	PGE_2 (ng/mL) −LPS	+LPS	TxB_2 (ng/mL) −calcium ionophore	+calcium ionophore
control	0.18	2.0	0.20	1.80
indomethacin		0.65		0.9
15		0.36		1.6

from mice (calculated w.r.t. C_{max}). The AUC trend in paw thickness vs time graph at different doses of the compound w.r.t. the control and standard clearly showed that treatment with **15** results in fast decrease of carrageenan-induced paw edema (Figure S109). A comparison of the PK data for celecoxib on rats at 5 mg kg^{-1} i.p. dose, showing $t_{1/2}$ 5.2 h and C_{max} 1.2 μg/mL achieved in 0.28 h (T_{max}) with $AUC_{0\text{-}t}$ 6.6 μg/mL·h,[52] indicates a better PK profile of **15** though we know celecoxib is an approved drug.

Plasma protein binding (PPB), water solubility, to be substrate of CYP3A4, and the Marine−Darby canine kidney (MDCK) parameters of **15** were also calculated[53] and compared with one of our previously reported potent molecule **2** and tepoxaline (Table 5). Due to the presence of four carboxyl groups, **15** is highly soluble in water which may decrease its rate of absorption from intestine into the blood. But given other favorable factors, poor drug absorption can be overcome by delivering the drug in the form of either nanoparticles or surfactant emulsion or its ester form. Advantageously, higher water solubility improved the permeability of the drug **15** to 1.59 nm/s in the MDCK model in comparison to 0.05 and 0.04 nm/s for **2** and tepoxaline, respectively. Remarkably, small PPB of **15** in comparison to **2** and tepoxaline may enable it to be a fast acting drug requiring a small dose. Higher PPB of the drug causes it to release slowly and may make it difficult to reach a therapeutic concentration, thus requiring higher drug dose. Hence, compound **15** seems relatively fast acting, and consequently, its small dose could be sufficient if given in appropriate formulation (also evident from the drug-response assay). Compound **2** being the substrate of CYP3A4 (enzyme responsible for drug metabolism in the liver) may get further reduced in concentration and also cause drug−drug interactions whereas **15** (similar to tepoxaline) is a weak substrate of CYP3A4. Overall, the pharmacokinetic

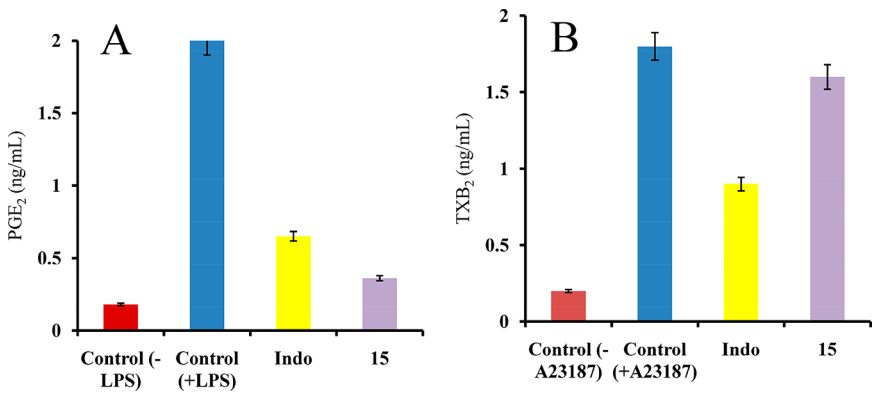

Figure 4. (A) PGE_2 and (B) TXB_2 inhibition in whole blood by indomethacin (1 μM) (abbreviated here as Indo) and compound **15** (1 μM). LPS and calcium ionophore were used as stimulants of COX-2 and COX-1, respectively.

https://doi.org/10.1021/acs.jmedchem.1c00880
J. Med. Chem. 2021, 64, 9550−9566

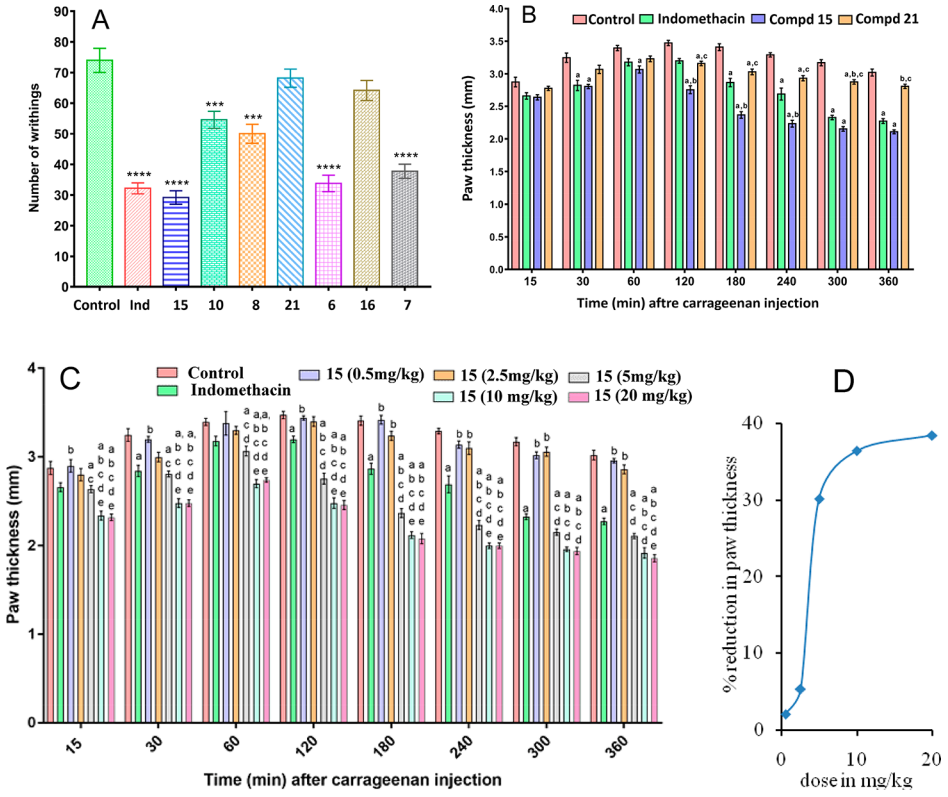

Figure 5. (A) Effect of compounds on acetic acid-induced writhings in Swiss albino mice. Data were analyzed by using one way ANOVA and expressed as mean ± SEM of six animals per group followed by Tukey's test. ***$p < 0.0002$ and ****$p < 0.0001$ compared to the control group. (B) Effect of compounds **15** and **21** at 5 mg kg^{-1} dose and (C) **15** on various doses on carrageenan-induced hind paw edema in Swiss albino mice. Data were analyzed by using one way ANOVA and expressed as mean ± SEM of six animals per group followed by Tukey's test. $^{a}p < 0.05$ compared to control group. $^{b}p < 0.05$ compared to indomethacin group. $^{c}p < 0.05$ compared to **15** (5/0.5 mg/kg). $^{d}p < 0.05$ compared to **15** (2.5 mg/kg). $^{e}p < 0.05$ compared to **15** (5 mg/kg). (D) Dose-dependent reduction in paw thickness (%) on treatment of mice with **15**.

Table 3. Percentage Decrease in Paw Edema on Treatment with Varied Doses of 15 (Dose-Response Assay)

S. No.	Dose (mg kg^{-1})	percentage decrease in paw edema (anti-inflammatory activity)
1	0.5	2.0
2	2.5	5.4
3	5	32.6
4	10	36.5
5	20	38.5

parameters of **15** are emerging superior to those of **2** and tepoxaline. The low log P (−3.26) and high total polar surface area (299.10) of **15** also comply with the high renal clearance features of a drug.

Isothermal Titration Calorimetry (ITC) Experiments. The binding interactions of the compounds with COX-1, COX-2, 5-LOX, and HSA (human serum albumin) were studied with the help of ITC experiments, and the data supported the biological results. The values of the thermodynamic parameters ΔH and ΔG (Table 6, Figure S110) indicated the exothermic and spontaneous binding of compound **15** with the enzymes. Apparently, compound **15** has better interactions with COX-2 in comparison to those with COX-1 and LOX. Compound was also found interacting with HSA- cordial for transportation and clearance in the biological system though many factors and several pathways are involved for the elimination of a compound.

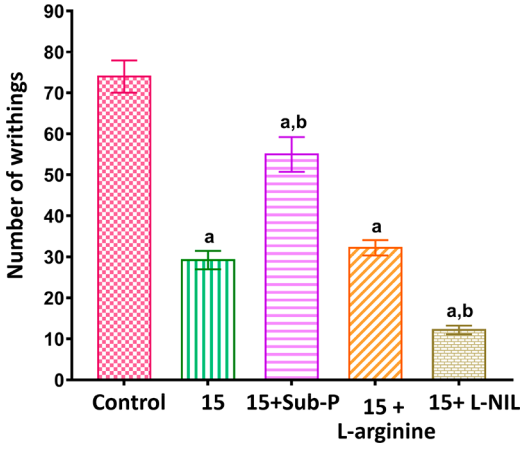

Figure 6. Effect of Sub-P, L-arginine, and L-NIL on the analgesic activity of compound **15** in an acetic acid-induced writhings test. Data were analyzed by using one way ANOVA and expressed as mean ± SEM of six animals per group followed by Tukey's test. $^{a}p < 0.05$ compared to control group, $^{b}p < 0.05$ compared to compound **15** group.

Molecular Modeling Studies. Docking calculations of the compounds were performed to determine their binding affinities with COX-2 and 5-LOX. Figure 8A shows the most potent compound **15** in the active site of COX-2. Three of the four carboxyl groups of the inhibitor formed H-bonds with the three very crucial amino acids of the COX-2 catalytic

https://doi.org/10.1021/acs.jmedchem.1c00880
J. Med. Chem. 2021, 64, 9550−9566

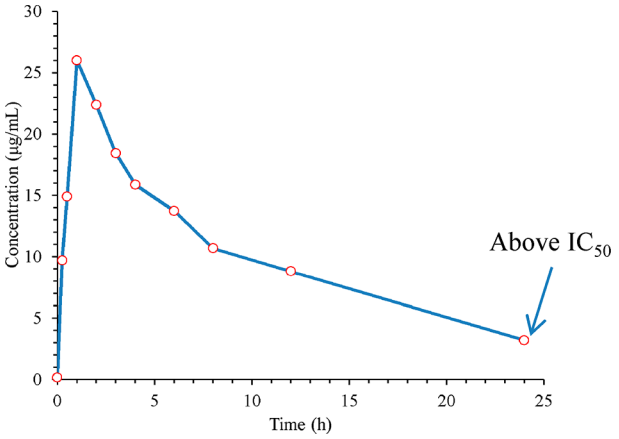

Figure 7. PK Profile for compound **15** in mice.

Table 4. PK Data of Compound 15

Parameter	Value
no. of animals	30
Dose level	10 mg kg^{-1}
$t_{1/2}$	8.74 h
T_{max}	1 h
C_{max}	26 μg/mL
AUC_{0-t}	241.27 μg/mL·h
Cl_obs	0.0355 (μg/mL)/h

Table 5. Predicted Pharmacokinetic Features of Compounds 2, 15, and Tepoxaline

Compound	PPB%	CYP3A4 substrate	MDCK (nm/s)	pure water solubility (mg/mL)
2	98	substrate	0.05	0.01
15	67	weakly	1.59	Freely
Tepoxaline	100	weakly	0.04	21.08

pocket,[54−59] i.e., Arg120, Tyr385, and Ser530 (Figure 8A, B). These H-bonds must strengthen the enzyme−ligand interactions and help in justifying the better COX-2 inhibitory activity of **15**. Apparently, the entrance as well as the interior part of the active site pocket was occupied by compound **15**, and its H-bond distances with Ser530 and Tyr385 were shorter and hence stronger than those shown by AA (Figure 8C). Remarkably, compound **15** occupied the same pocket of COX-2 where AA sits but with the additional advantage of H-bonding, thus supporting the hypothesis made in the design of the molecules. Compound **15** was certainly better fit and more interactive in the COX-2 active site in comparison to one of our previous compound **2** (Figure 2, Figure 8D) as well as COX-2/LOX inhibitor tepoxaline (Figure 2; Figure 8E, F) though the IC_{50} value of **15** for COX-2 was slightly higher than that of **2**. Compound **6**, the ester precursor of **15**, exhibited only $\pi-\pi$ interactions with Tyr355 and Arg120 (Figure S111A, B). Compound **7** interacted with Arg120 and Tyr115 at the entry point and not in the interior of the cavity (Figure S112). Compounds **8−14** and **19−23** as well as their acid counterparts partially enter into the active site of the enzyme and did not show H-bond interactions with any of the residues there.

Since compound **15** also appeared potent for LOX, its docking in 5-LOX showed that it fits in the active site of the enzyme and coordinates with Fe^{2+} through the two carboxyl groups (Figure 9A, B). Another carboxyl group was H-bonded to Phe177. Additionally, the triazole rings of **15** were engaged in $\pi-\pi$ and cation$-\pi$ interactions with Phe177 and Lys409, respectively. It was observed that compound **15** exhibits more number of interactions with Fe^{2+} and hence better coordination than that shown by tepoxaline (Figure 9C, D). Compounds **6−10** and **21−23** also exhibited appreciable interactions with the active site amino acid residues of 5-LOX (Figure S113−S118). Most of these compounds were coordinating with Fe^{2+} that may be the reason for their LOX inhibitory activities. As a result, we found a good correlation between the experimental and calculated data suggesting the stereoelectronic compliance of the drug/compound with the target enzyme for its higher efficacy. Only compound **15** in this series showed unique interactions with both COX-2 and LOX, even appreciably better than those exhibited by the reported drug tepoxaline. It seems that the engaging of carboxyl groups in H-bonding with COX-2 and coordinating with Fe^{2+} in LOX enable a **15** dual COX-2/LOX inhibitor.

CONCLUSIONS

Chronic inflammation is a highly debilitating physiological stage that is implicated in a number of diseases. Among the various cellular targets of the anti-inflammatory agents, the COX-2 and LOX inhibitors are the most extensively explored but the side effects associated with these compounds are the major bottlenecks in their transformation to clinical drugs. Even the clinically available drugs such as celecoxib (Celebrex) (COX-2 inhibitor) and tepoxaline (Zubrin) (COX-2, LOX inhibitor) suffer from side effects. Since the interaction/binding of the inhibitor with its cellular target is important for the efficacy of the compound, based on this concept, here, we report a new series of COX-2, LOX dual inhibitors. Imparting the flexibility and stereochemical attributes to the molecules, tartarate based acyclic compounds were developed as a probable replacement of the usual heterocyclic-template mono/biaryl substituted inhibitors of the AA pathway. As shown by the combined results of molecular modeling studies and the in vitro and in vivo experiments, compound **15** is a promising candidate for anti-inflammatory drugs. This compound exhibited the IC_{50} values 4 nM and 7 nM for COX-2 and LOX, respectively. In contrast to the conventional COX-2/LOX inhibitors, compound **15** does not carry a single phenyl ring that may render its safe metabolism. Desirably, the selectivity index of compound **15** for COX-2 over COX-1 was less than that of highly selective celecoxib but more than

Table 6. ITC Data for the Binding of Compound 15 with the Enzymes

Physical parameters	COX-1	COX-2	5-LOX	HSA
K_a (M^{-1})	$(1.64 \pm 0.49) \times 10^3$	$(6.07 \pm 0.63) \times 10^5$	$(1.33 \pm 0.12) \times 10^5$	$(1.18 \pm 0.66) \times 10^4$
ΔH (kJ/mol)	-25.12×10^2	−43.73	−41.81	-11.05×10^2
$T\Delta S$(kJ/mol)	-24.91×10^2	−10.75	−12.53	-10.81×10^2
ΔG (kJ/mol)	−21.00	−32.98	−29.28	−23.26

https://doi.org/10.1021/acs.jmedchem.1c00880
J. Med. Chem. 2021, 64, 9550−9566

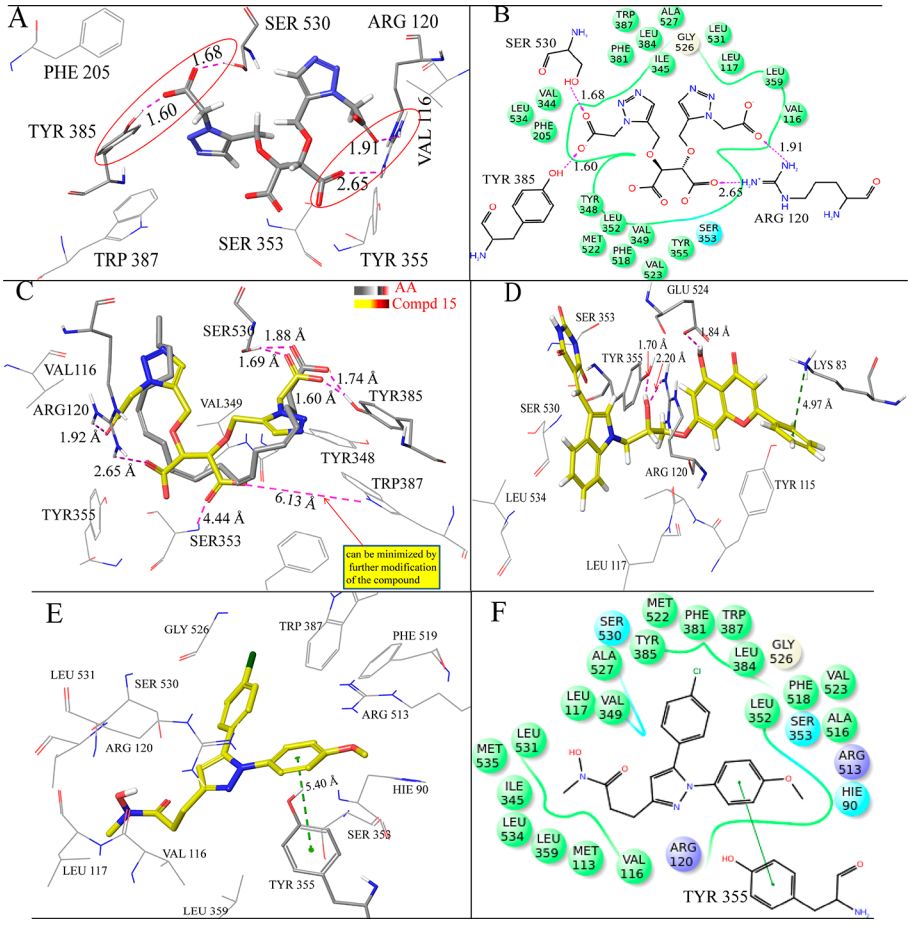

Figure 8. (A) 3D representation of compound **15** docked in the COX-2 (1CVU) active site. (B) 2D interaction diagram of compound **15** with amino acid residues lining the active site of COX-2. (C) Compound **15** (in yellow-red) docked in COX-2 showing overlapping with AA (gray-red) cocrystallized with the enzyme. (D) Compound **2** docked in COX-2. (E and F) Tepoxaline docked in the active site of COX-2 representing 3D and 2D views. Nonpolar H's are removed for clarity.

nonselective indomethacin, that may help compound **15** to overcome the COX-2/1 selectivity related limitations of the reported anti-inflammatory drugs. Furthermore, compound **15** does not show in vivo toxicity up to 300 mg kg^{-1} dose and exhibited significant reversal of inflammation and analgesia in the treated Swiss albino mice. Our results suggest that the novel tartarate−1,2,3-triazole carboxylate based COX-2/LOX inhibitors deserve further investigations as potential anti-inflammatory agents.

EXPERIMENTAL SECTION

General. Melting points were determined in capillaries using a VEGGO digital melting point apparatus and are uncorrected. ^{1}H NMR spectra were recorded on Bruker 500 and JEOL 400 MHz NMR spectrometers with the corresponding recording of ^{13}C NMR spectra respectively at 125 and 100 MHz. $CDCl_3$ and DMSO-d_6 were used as the solvents with TMS as the internal reference. Chemical shifts are given in ppm and J values in hertz (Hz). For ^{13}C and DEPT-135 NMR spectra, positive signals correspond to CH_3 and CH carbons, and negative signals correspond to CH_2 carbons. Mass spectra were recorded on a Bruker micrOTOF QII mass spectrometer for high resolution mass spectra (HRMS). IR spectra were recorded on a Varian 660 IR spectrometer. Reactions were monitored by thin layer chromatography (TLC) on glass plates coated with silica gel GF-254. Column chromatography was performed on 60−120 mesh silica. Percentage purity 98% was confirmed with the help of a ^{1}H NMR spectrum (Figure S119) as reported earlier.[60] The purity of the compounds were also checked by LC-MS for which 2 μL of sample compound (dissolved in methanol) was injected to the column (Kromasil Silica, 5 μ, 250 mm × 4.6 mm, 60 Å) by autosampler of Dionex Ultimate 3000 connected to a mass spectrometer. An isocratic mobile phase consisting acetonitrile and water (composition mentioned for each compound along with the LC-MS in SI) was used with the flow rate of 0.2 mL/min. The purity of the sample was calculated with the following formula, and it is given along with the LC-MS of each compound in the SI.

$$MS\ Sample\ Purity = \frac{Area\ of\ Single\ Peak\ (summed\ EIC)}{Area\ of\ All\ Integrated\ Peaks\ (TIC)} \times 100 \quad (1)$$

General Procedure for Synthesis of Compounds. *Procedure A.* To a suspension of sodium hydride (0.77 g, 60% in mineral oil, 0.019 mol) in THF (20 mL), a solution of L-diethyltartarate (2.09 g, 0.01 mol) in THF (30 mL) was added dropwise over 30 min with stirring at 0 °C. After the mixture was stirred for 1 h at 0 °C, tetrabutylammonium bromide (0.074 g, 0.002 mol) and 18-crown-6 (6 mg, 0.022 mmol) (catalytic amount) were added in one portion. Propargyl bromide (2.37 g, 0.02 mol) was added dropwise over 30 min at 0 °C. The resulting mixture was stirred for 12 h at room temperature, quenched with 1 N aqueous HCl, poured into water, and extracted with three portions of ether. The combined organic layers were washed with aqueous $NaHCO_3$ and brine, dried over Na_2SO_4, and concentrated under vacuum to give the crude product which was purified by column chromatography using ethyl acetate and hexane as eluent to obtain compounds **4** and **5** in 40% and 15% yield, respectively.

https://doi.org/10.1021/acs.jmedchem.1c00880
J. Med. Chem. 2021, 64, 9550−9566

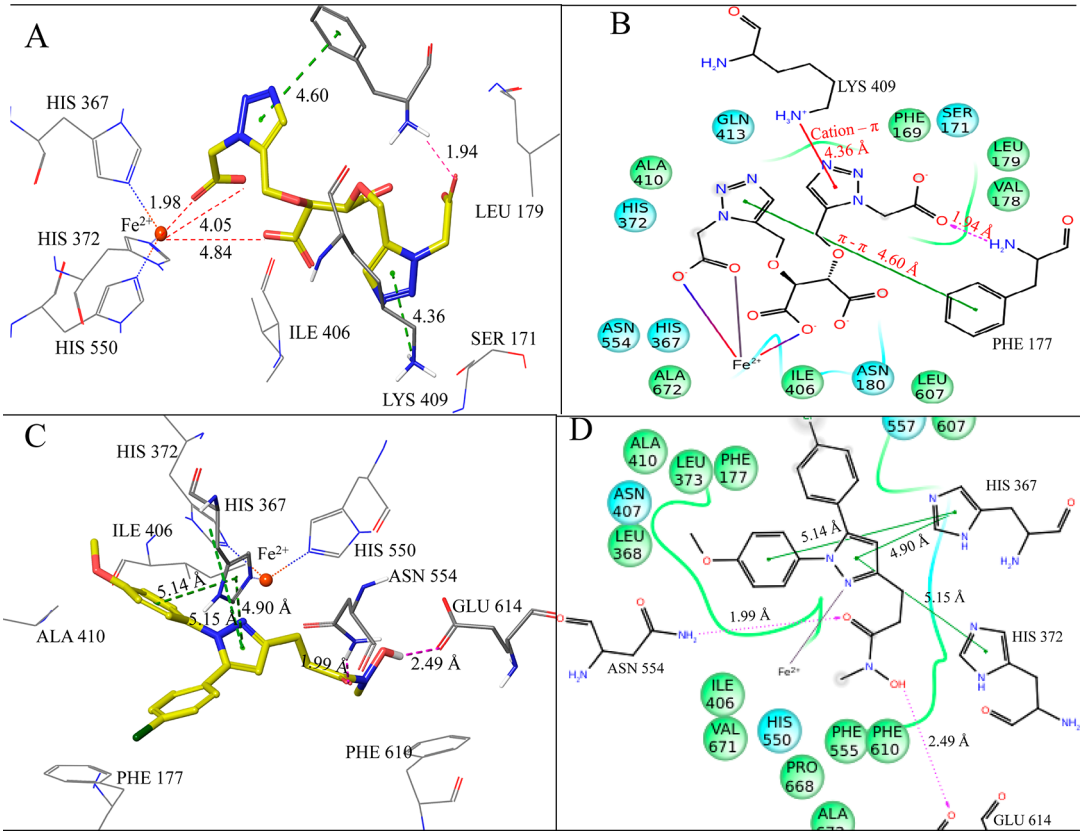

Figure 9. (A) 3D representation of **15** docked in the 5-LOX (3V99) active site. (B) 2D interaction diagram of compound **15** with amino acid residues lining the active site of 5-LOX. Molecular docking of tepoxaline in the active site pocket of 5-LOX representing (C) 3D and (D) 2D views of interactions. Nonpolar H's are removed for clarity.

Procedure B. To a solution of *S*-binol (500 mg, 1.7 mmol) in acetone, anhydrous potassium carbonate (720 mg, 5.20 mmol) and propargyl bromide (620 mg, 5.21 mmol) were added. The reaction mixture was allowed to stir at 60 °C for 16 h. After completion of the reaction (TLC), the reaction mixture was filtrated and the filtrate was evaporated under reduced pressure. The residue was purified by recrystallization (petroleum ether/EtOAc) to give compound **18** in 95% yield.

Procedure C. Preparation of Azides of Amino Acid. Ester of L-amino acid (1 mmol) was dissolved in methanol followed by the addition of anhydrous potassium carbonate (1.19 mmol), imidazole sulphonyl azide hydrochloride (ISA.HCl) (1.19 mmol), and $CuSO_4$ (1 mol %). The reaction mixture was stirred for 6 h at room temperature. After the completion of the reaction, it was quenched with water and extracted with ethyl acetate (3 × 25 mL). The combined organic layers were separated, dried over Na_2SO_4, and concentrated under vacuum to obtain the crude product which was then purified by column chromatography using ethyl acetate/hexane as eluent. All the amino acid azides were procured in 85−90% yield.

Procedure D. Preparation of Ethyl 2-Azidoacetate. To the solution of ethyl bromoacetate (2.00 g, 12 mmol) in acetone (12 mL), sodium azide (2.73 g, 42 mmol) in water (12 mL) was added at 0 °C under vigorous agitation. This reaction mixture was then warmed to room temperature and heated at 60 °C overnight. The aqueous phase was washed with dichloromethane (DCM) (3 × 15 mL). The organic layers were combined and washed with a solution (10%) of sodium bicarbonate (20 mL) and water (20 mL). Then the organic layer was dried on Na_2SO_4, and the solvent was evaporated under vacuum to afford ethyl 2-azidoacetate as a pale yellow liquid. No further purification was done of the crude product.

Procedure E. Compound **4**/**5**/**18** (1 mmol) was dissolved in ethanol. To this solution, sodium ascorbate (5 mol %) and $CuSO_4 \cdot 5H_2O$ (2 mol %) dissolved in water and the azide (2.1 mmol) taken in ethanol were added in sequence. The reaction mixture was stirred at room temperature and monitored with TLC. After the completion of the reaction, it was diluted with distilled water and extracted with ethyl acetate. Ethyl acetate was distilled off under reduced pressure to give a thick oil/solid which was purified with column chromatography using a mixture of ethyl acetate and hexane as eluent to isolate the product. Compounds **6**−**10**, **11**−**14**, and **19**−**23** were procured with 70−90% yield. For compounds **11**−**14**, 1.1 mmol of the azide was used.

*Procedure F. Hydrolysis of Compounds **6** and **9**.* To the solution of compound **6**/**9** (1 mmol) in acetone−water (3:2), 1 N NaOH (4 mmol) was added. The reaction mixture was allowed to stir at room temperature until completion (TLC). After completion, acetone was evaporated under vacuum and the pH of the water layer was adjusted to acidic with 1 N HCl followed by extraction with ethyl acetate to obtain desired product **16** after removing the ethyl acetate. However, in the case of hydrolysis of **6**, the desired compound **15** was isolated from the water layer by washing with warm acetone.

*Diethyl (2R,3R)-2,3-Bis(prop-2-yn-1-yloxy)succinate (**4**).* Compound **4** was synthesized according to general procedure A using L-diethyl tartarate and propargyl bromide and purified by column chromatography using ethyl acetate−hexane (0.5:9.5 v/v) as eluent. Thick transparent oil, yield 40%. ^{1}H NMR (400 MHz, $CDCl_3$) δ 1.33 (t, J = 7.3 Hz, 6H, CH_3), 2.45 (t, J = 2.5 Hz, 2H, CH_2), 4.25−4.31 (m, 4H, CH_2), 4.34−4.35 (m, 2H, CH_2), 4.41−4.42 (m, 1H, CH of CH_2), 4.45−4.46 (m, 1H, CH of CH_2), 4.77 (s, 2H, CH). ^{13}C NMR (100 MHz, $CDCl_3$) δ 14.2 (+ve, CH_3), 57.9 (−ve, CH_2), 61.6 (−ve, CH_2), 75.7 (+ve, CH), 76.6 (+ve, CH), 78.32 (C), 168.3 (C ═O). HRMS (microTOF-QII, MS, ESI): Calcd for $C_{14}H_{18}O_6$ ([M + Na]$^+$) 305.0996, found 305.0994.

*Diethyl (2R,3R)-2-Hydroxy-3-(prop-2-yn-1-yloxy)succinate (**5**).* Compound **5** was synthesized according to general procedure A using L-diethyl tartarate and propargyl bromide. Sticky, transparent

https://doi.org/10.1021/acs.jmedchem.1c00880
J. Med. Chem. 2021, 64, 9550−9566

liquid, yield 15%. ^{1}H NMR (500 MHz, $CDCl_3$) δ 1.31−1.34 (m, 6H, 2 × CH_3), 2.44 (t, J = 2.32 Hz, 1H, CH), 3.13 (d, J = 7.09 Hz, 1H, OH), 4.28−4.32 (m, 5H, $2CH_2$ + 1H of CH_2), 4.40−4.44 (m, 1H, 1H of CH_2), 4.61−4.62 (m, 1H, CH), 4.63−4.64 (m, 1H, CH). ^{13}C NMR (125 MHz, $CDCl_3$) δ 14.1 (+ve, CH_3), 57.7 (−ve, CH_2), 61.7 (−ve, CH_2), 62.2 (−ve, CH_2), 72.0 (+ve, CH), 75.6 (+ve, CH), 76.8 (+ve, CH), 78.32 (C), 168.3 (C═O).

*Diethyl (2R,3R)-2,3-Bis((1-(2-ethoxy-2-oxoethyl)-1H-1,2,3-triazol-5-yl)methoxy)succinate (**6**).* Compound **6** was synthesized according to general procedure E using compound **4** and ethyl bromoacetate azide and purified by column chromatography with ethyl acetate−hexane (6:4). Thick oil, yield 73%. IR (ATR): 3145, 2981, 2094, 1744, 1558, 1468, 1371, 1267, 1207, 1095, 1021, 872, 797, 708, 581, 447 cm^{-1}. $[\alpha]_D^{25}$ = +40° (0.4, $CHCl_3$). ^{1}H NMR (400 MHz, $CDCl_3$) δ 1.24 (t, J = 7.1 Hz, 6H, CH_3), 1.30 (t, J = 7.3 Hz, 6H, CH_3), 4.14−4.21 (m, 4H, CH_2), 4.23−4.29 (m, 4H, CH_2), 4.56 (s, 2H, CH), 4.68−4.71 (m, 2H, CH_2), 4.71−4.96 (m, 2H, CH_2), 5.12−5−13 (m, 4H, CH_2), 7.73 (s, 2H, ArH). ^{13}C NMR (100 MHz, $CDCl_3$) δ 14.0 (+ve, CH_3), 14.1 (+ve, CH_3), 50.8 (−ve, CH_2), 61.5 (−ve, CH_2), 62.4 (−ve, CH_2), 64.9 (−ve, CH_2), 78.8 (+ve, CH), 124.5 (+ve, ArCH), 144.6 (ArC), 166.1 (C═O), 168.8 (C═O). HRMS (microTOF-QII, MS, ESI): Calcd for $C_{22}H_{32}O_{10}N_6$ ([M + Na]$^+$) 563.2072, found 563.2055.

*Diethyl (2R,3R)-2,3-Bis((1-((S)-3-hydroxy-1-methoxy-1-oxopropan-2-yl)-1H-1,2,3-triazol-5-yl)methoxy)succinate (**7**).* Compound **7** was synthesized according to general procedure E using compound **4** and (*S*)-serine methyl ester azide. It was purified by column chromatography using ethyl acetate−hexane (7:3) eluent. Thick oil, yield 75%. IR (ATR): 3459, 3153, 2959, 2355, 2117, 1744, 1558, 1446, 1371, 1274, 1207, 1095, 1021, 775, 700, 596, 492 cm^{-1}. $[\alpha]_D^{25}$ = +87.5° (0.4, $CHCl_3$). ^{1}H NMR (400 MHz, $CDCl_3$). δ 1.26−1.32 (m, 6H, CH_3), 3.80−3.82 (s, 6H, 2 × OCH_3), 4.14−4.22 (m, 6H, CH_2), 4.32−4.37 (m, 2H, CH_2), 4.43−4.46 (m, 2H, CH), 4.60−4.66 (m, 2H, CH_2), 4.87−4.90 (m, 2H, CH_2), 5.47−5.49 (m, 2H, CH), 7.94 (s, 2H, ArH). ^{13}C NMR (100 MHz, $CDCl_3$) δ 14.1 (+ve, CH_3), 53.2 (+ve, OCH_3), 62.1 (−ve, CH_2), 62.8 (−ve, CH_2), 64.5 (+ve, CH), 64.6 (−ve, CH_2), 78.3 (+ve, CH), 124.9 (+ve, ArCH), 143.5 (ArC), 167.4 (C═O), 169.5 (C═O). HRMS (microTOF-QII, MS, ESI): Calcd for $C_{22}H_{32}O_{12}N_6$ ([M + Na]$^+$) 595.1970, found 595.1979.

*Diethyl (2R,3R)-2,3-Bis((1-((S)-3-(4-hydroxyphenyl)-1-methoxy-1-oxopropan-2-yl)-1H-1,2,3-triazol-5-yl)methoxy)succinate (**8a**).* Compound **8a** was synthesized according to general procedure E using compound **4** and (*S*)-tyrosine methyl ester azide. Crude product was purified by column chromatography with ethyl acetate−hexane (7:3). Thick oil, yield 72%. IR (ATR): 3451, 3145, 3019, 2094, 1744, 1610, 1520, 1446, 1371, 1267, 1207, 1013, 827, 752, 596, 544 cm^{-1}. $[\alpha]_D^{25}$ = −7.50° (0.4, $CHCl_3$). ^{1}H NMR (400 MHz, $CDCl_3$) δ 1.20−1.28 (m, 6H, CH_3), 3.36−3.39 (m, 4H, CH_2), 3.78 (s, 6H, OCH_3), 4.11−4.16 (m, 4H, CH_2), 4.44 (s, 2H, CH), 4.57−4.60 (m, 2H, CH_2), 4.81−4.84 (m, 2H, CH_2), 5.47−5.51 (m, 2H, CH), 6.67 (d, J = 8.7 Hz, 4H, ArH), 6.75 (d, J = 8.7 Hz, 4H, ArH), 7.55 (s, 2H, ArH). ^{13}C NMR (100 MHz, $CDCl_3$) δ 14.1 (+ve, CH_3), 38.0 (−ve, CH_2), 53.1 (+ve, OCH_3), 61.6 (−ve, CH_2), 64.3 (+ve, CH), 64.5 (−ve, CH_2), 78.9 (+ve, CH), 115.9 (+ve, ArCH), 124.1 (+ve, ArCH), 125.5 (ab, ArC), 130.0 (+ve, ArCH), 143.7 (ab, ArC), 155.9, (ab, ArC), 168.5 (C═O), 168.9 (C═O). HRMS (microTOF-QII, MS, ESI): Calcd for $C_{34}H_{40}O_{12}N_6$ ([M + Na]$^+$) 747.2592, found 747.2589.

*Diethyl (2R,3R)-2-((1-((R)-3-(4-hydroxyphenyl)-1-methoxy-1-oxopropan-2-yl)-1H-1,2,3-triazol-5-yl)methoxy)-3-((1-((S)-3-(4-hydroxyphenyl)-1-methoxy-1-oxopropan-2-yl)-1H-1,2,3-triazol-5-yl)methoxy)succinate (**8g/h**).* Compound **8g**/**h** was synthesized according to general procedure E using compound **4** and (*S*)-tyrosine methyl ester azide and (*R*)-tyrosine methyl ester azide. Thick oil, yield 54%. $[\alpha]_D^{25}$ = −18° (0.4, $CHCl_3$).

*Diethyl (2R,3R)-2,3-Bis((1-((S)-1-methoxy-1-oxo-3-phenypropan-2-yl)-1H-1,2,3-triazol-5-yl)methoxy)succinate (**9**).* Compound **9** was synthesized according to general procedure E using compound **4** and (*S*)-phenylalanine methyl ester azide. It was purified by column chromatography using ethyl acetate−hexane (6:4) as eluent. Thick oil, yield 74%. IR (ATR): 3138, 2952, 2124, 1744, 1453, 1371, 1267, 1200, 1103, 1021, 812, 752, 506, 454 cm^{-1}. $[\alpha]_D^{25}$ = −32.5° (0.4, $CHCl_3$). ^{1}H NMR (400 MHz, $CDCl_3$) δ 1.19−1.27 (m, 6H, CH_3), 3.40−3.56 (m, 4H, CH_2), 3.73 (s, 6H, OCH_3), 4.07−4.19 (m, 4H, CH_2), 4.51−4.52 (m, 2H, CH), 4.64−4.67 (m, 2H, CH_2), 4.89−4.92 (m, 2H, CH_2), 5.49−5.53 (m, 2H, CH), 7.04−7.08 (m, 5H, ArH), 7.21−7.25 (m, 5H, ArH), 7.71 (s, 2H, ArH). ^{13}C NMR (100 MHz, $CDCl_3$) δ 14.2 (+ve, CH_3), 38.8 (−ve, CH_2), 53.1 (+ve, OCH_3), 61.5 (−ve, CH_2), 64.1 (+ve, CH), 65.0 (−ve, CH_2), 78.8 (+ve, CH), 123.1 (+ve, ArCH), 127.6 (+ve, ArCH), 128.9 (+ve, ArCH), 129.0 (+ve, ArCH), 134.8 (ab, ArC), 144.2 (ab, ArC), 168.6 (C═O), 168.8 (C═O). HRMS (microTOF-QII, MS, ESI): Calcd for $C_{34}H_{40}O_{10}N_6$ ([M + H]$^+$) 693.2879, found 693.2902.

*Diethyl (2R,3R)-2,3-Bis((1-((S)-3-(1H-indol-3-yl)-1-methoxy-1-oxopropan-2-yl)-1H-1,2,3-triazol-5-yl)methoxy)succinate (**10**).* Compound **10** was synthesized according to general procedure E using compound **4** and (*S*)-tryptophan methyl ester azide. Column chromatography using ethyl acetate−hexane (6:4) was performed for the purification. Thick oil, yield 72%. IR (ATR): 3391, 3138, 2952, 2594, 2355, 2079, 1744, 1438, 1341, 1267, 1200, 1095, 1013, 857, 745, 603, 506 cm^{-1}. $[\alpha]_D^{25}$ = −5.0° (0.4, $CHCl_3$). ^{1}H NMR (400 MHz, $CDCl_3$) δ 1.16−1.28 (m, 6H, CH_3), 3.52−3.66 (m, 4H, CH_2), 3.77 (s, 6H, OCH_3), 3.96−4.04 (m, 2H, CH_2), 4.08−4.16 (m, 2H, CH_2), 4.45−4.46 (m, 2H, CH), 4.57−4.60 (m, 2H, CH_2), 4.84−4.88 (m, 2H, CH_2), 5.54−5.58 (m, 2H, CH), 6.52 (d, J = 2.3 Hz, 2H, ArH), 7.10−7.18 (m, 4H, ArH), 7.31 (d, J = 7.8 Hz, 2H, ArH), 7.53−7.54 (m, 4H, ArH), 8.70 (br, 2H, NH). ^{13}C NMR (100 MHz, $CDCl_3$) δ 14.0 (+ve, CH_3), 28.9 (−ve, CH_2), 53.1 (+ve, OCH_3), 61.7 (−ve, CH_2), 63.1 (+ve, CH), 64.5 (−ve, CH_2), 78.8 (+ve, CH), 107.8 (ab, ArC), 111.6 (+ve, ArCH), 117.8 (+ve, ArCH), 119.5 (+ve, ArCH), 122.0 (+ve, ArCH), 123.8 (+ve, ArCH), 124.2 (+ve, ArCH), 126.5 (ab, ArC), 136.0 (ab, ArC), 143.5 (ab, ArC), 168.9 (C═O), 169.03 (C═O). HRMS (microTOF-QII, MS, ESI): Calcd for $C_{38}H_{42}O_{10}N_8$ ([M + Na]$^+$) 793.2916, found 793.2925.

*Diethyl (2R,3R)-2-((1-(2-Ethoxy-2-oxoethyl)-1H-1,2,3-triazol-5-yl)methoxy)-3-hydroxysuccinate (**11**).* Compound **11** was synthesized according to general procedure E using compound **5** and ethyl bromo acetate azide. It was purified by column chromatography with ethyl acetate−hexane (4:6). Thick oil, yield 76%. IR (ATR): 3503, 3145, 2981, 2355, 2087, 1744, 1558, 1468, 1371, 1207, 1140, 1021, 864, 797, 708, 581, 447 cm^{-1}. ^{1}H NMR (400 MHz, $CDCl_3$) δ 1.24 (t, J = 7.1 Hz, 3H, CH_3), 1.29−1.34 (m, 6H, CH_3), 4.11−4.20 (m, 1H, CH of CH_2), 4.21−4.32 (m, 5H, CH + CH_2), 4.51 (d, J = 2.3 Hz, 1H, CH), 4.62 (d, J = 2.3 Hz, 1H, CH), 4.66−4.69 (m, 1H, CH of CH_2), 4.92−4.95 (m, 1H, CH of CH_2), 5.15 (s, 2H, CH_2), 7.72 (s, 1H, ArH). ^{13}C NMR (100 MHz, $CDCl_3$) δ 14.15 (+ve, CH_3), 14.18 (+ve, CH_3), 14.2 (+ve, CH_3), 50.9 (−ve, CH_2), 61.8 (−ve, CH_2), 62.3 (−ve, CH_2), 62.5 (−ve, CH_2), 64.5 (−ve, CH_2), 72.3 (+ve, CH), 78.9 (+ve, CH), 124.5 (+ve, ArCH), 144.6 (ArC), 166.1 (C═O), 169.1 (C═O), 171.1 (C═O). HRMS (microTOF-QII, MS, ESI): Calcd for $C_{15}H_{23}O_8N_3$ ([M + Na]$^+$) 396.1377, found 396.1394.

*Diethyl (2R,3R)-2-Hydroxy-3-((1-((S)-3-hydroxy-1-methoxy-1-oxopropan-2-yl)-1H-1,2,3-triazol-5-yl)methoxy)succinate (**12**).* Compound **12** was synthesized according to general procedure E using compound **5** and (*S*)-serine methyl ester azide. Crude product was purified by column chromatography with ethyl acetate−hexane (4:6). Thick oil, yield 73%. IR (ATR): 3481, 2959, 2087, 1736, 1446, 1371, 1200, 1095, 1021, 857, 700, 596, 492 cm^{-1}. ^{1}H NMR (400 MHz, $CDCl_3$) δ 1.27 (t, J = 7.1 Hz, 3H, CH_3), 1.33 (t, J = 7.1 Hz, 3H, CH_3), 3.82 (s, 3H, OCH_3), 4.14−4.21 (m, 3H, CH_2 + CH of CH_2), 4.26−4.31 (m, 2H, CH_2), 4.35−4.39 (m, 1H, CH of CH_2), 4.47 (d, J = 2.3 Hz, 1H, CH), 4.61 (d, J = 2.3 Hz, 1H, CH), 4.63−4.66 (m, 1H, CH of CH_2), 4.89−4.92 (m, 1H, CH of CH_2), 5.47−5.50 (m, 1H, CH), 7.96 (s, 1H, ArH). ^{13}C NMR (100 MHz, $CDCl_3$) δ 14.0 (+ve, CH_3), 14.1 (+ve, CH_3), 53.2 (+ve, OCH_3), 61.8 (−ve, CH_2), 62.3 (−ve, CH_2), 62.6 (−ve, CH_2), 64.40 (−ve, CH_2), 64.45 (+ve, CH), 72.41 (+ve, CH), 78.68 (+ve, CH), 124.7 (ArCH), 143.6 (ArC), 167.4 (C═O), 169.2 (C═O), 171.2 (C═O). HRMS (microTOF-

https://doi.org/10.1021/acs.jmedchem.1c00880
J. Med. Chem. 2021, 64, 9550−9566

QII, MS, ESI): Calcd for $C_{15}H_{23}O_9N_3$ ([M + Na]$^+$) 412.1327, found 412.1333.

*Diethyl (2R,3R)-2-Hydroxy-3-((1-((S)-3-(4-hydroxyphenyl)-1-methoxy-1-oxopropan-2-yl)-1H-1,2,3-triazol-5-yl)methoxy)succinate (**13**).* Compound **13** was synthesized according to general procedure E using compound **5** and (*S*)-tyrosine methyl ester azide and purified by column chromatography with ethyl acetate−hexane (1:1). Thick oil, yield 73%. IR (ATR): 3459, 3145, 2981, 2355, 2087, 1736, 1520, 1446, 1371, 1200, 1095, 1013, 834, 700, 544 cm^{-1}. ^{1}H NMR (400 MHz, $CDCl_3$) δ 1.21 (t, J = 7.1 Hz, 3H, CH_3), 1.31 (t, J = 7.2 Hz, 3H, CH_3), 3.33−3.43 (m, 2H, CH_2), 3.78 (s, 3H, OCH_3), 4.05−4.13 (m, 1H, CH of CH_2), 4.15−4.22 (m, 1H, CH of CH_2), 4.25−4.30 (m, 2H, CH_2), 4.46 (d, J = 2.3 Hz, 1H, CH), 4.57−4.62 (m, 2H, CH of CH_2 + CH), 4.86−4.89 (m, 1H, CH of CH_2), 5.49−5.52 (m, 1H, CH), 6.70 (d, J = 8.2 Hz, 2H, ArH), 6.84 (d, J = 8.7 Hz, 2H, ArH), 7.61 (s, 1H, ArH). ^{13}C NMR (100 MHz, $CDCl_3$) δ 14.10 (+ve, CH_3), 14.15 (+ve, CH_3), 38.0 (−ve, CH_2), 53.1 (+ve, OCH_3), 61.8 (−ve, CH_2), 62.3 (−ve, CH_2), 64.3 (+ve, CH), 64.4 (−ve, CH_2), 72.2 (+ve, CH), 79.0 (+ve, CH), 115.8 (ArCH), 123.3 (ArCH), 126.0 (ArC), 130.0 (ArCH), 143.8 (ArC), 155.5 (ArC), 168.5 (C═O), 169.1 (C═O), 171.1 (C═O). HRMS (microTOF-QII, MS, ESI): Calcd for $C_{21}H_{27}O_9N_3$ ([M + Na]$^+$) 488.1640, found 488.1635.

*Diethyl (2R,3R)-2-hydroxy-3-((1-((S)-1-methoxy-1-oxo-3-phenylpropan-2-yl)-1H-1,2,3-triazol-5-yl)methoxy)succinate (**14**).* Compound **14** was synthesized according to general procedure E using compound **5** and (*S*)-phenyalanine methyl ester azide and purified by column chromatography with ethyl acetate−hexane (3:7). Thick oil, yield 75%. IR (ATR): 3145, 2952, 2355, 2117, 1744, 1625, 1558, 1453, 1371, 1274, 1177, 820, 752, 566, 506, 462 cm^{-1}. ^{1}H NMR (400 MHz, $CDCl_3$) δ 1.22 (t, J = 7.3 Hz, 3H, CH_3), 1.32 (t, J = 7.1 Hz, 3H, CH_3), 3.42−3.56 (m, 2H, CH_2), 3.75 (s, 3H, OCH_3), 4.06−4.14 (m, 1H, CH of CH_2), 4.16−4.23 (m, 1H, CH of CH_2), 4.25−4.31 (m, 2H, CH_2), 4.46 (d, J = 2.5 Hz, 1H, CH), 4.60−4.63 (m, 2H, CH of CH_2 + CH), 4.89 (m, 1H, CH of CH_2), 5.52−5.55 (m, 1H, CH), 7.03−7.06 (m, 2H, ArH), 7.22−7.29 (m, 3H, ArH), 7.66 (s, 1H, ArH). ^{13}C NMR (100 MHz, $CDCl_3$) δ 14.12 (+ve, CH_3), 14.17 (+ve, CH_3), 38.7 (−ve, CH_2), 53.2 (+ve, OCH_3), 61.7 (−ve, CH_2), 62.3 (−ve, CH_2), 64.1 (+ve, CH), 64.6 (−ve, CH_2), 72.3 (+ve, CH), 78.9 (+ve, CH), 123.0 (ArCH), 127.6 (ArCH), 128.9 (ArCH), 134.6 (ArC), 144.0 (ArC), 168.5 (C═O), 169.0 (C═O), 171.0 (C═O). HRMS (microTOF-QII, MS, ESI): Calcd for $C_{21}H_{27}O_8N_3$ ([M + Na]$^+$) 472.1690, found 472.1664.

*(2R,3R)-2,3-Bis((1-(carboxymethyl)-1H-1,2,3-triazol-5-yl)-methoxy)succinic acid (**15**).* Compound **15** was synthesized according to general procedure F using compound **6** and 1N NaOH. Creamish solid, yield 78%. mp 132−34 °C. IR (ATR): 3384, 3145, 2892, 2363, 1722, 1625, 1222, 812, 641 cm^{-1}. ^{1}H NMR (500 MHz, DMSO-d_6) δ 4.44 (s, 2H, 2xCH), 4.49−4.53 (m, 2H, CH_2), 4.75−4.77 (m, 2H, CH_2), 5.25 (s, 4H, 2 × CH_2), 7.98 (s, 2H, ArH). ^{13}C NMR (125 MHz, DMSO-d_6) δ 50.9 (−ve, CH_2), 64.2 (−ve, CH_2), 78.6 (+ve, CH), 125.9 (+ve, ArCH), 143.8 (ArC), 169.1 (C═O), 170.7 (C═O). HRMS (microTOF-QII, MS, ESI): Calcd for $C_{14}H_{16}O_{10}N_6$ ([M − H]$^-$) 427.0844, found 427.0853.

*(2R,3R)-2,3-Bis((1-((S)-1-carboxy-2-phenylethyl)-1H-1,2,3-triazol-5-yl)methoxy)succinic acid (**16**).* Compound **16** was synthesized according to general procedure F using compound **9** and 1N NaOH. Creamish solid, yield 80%. mp 150−153 °C. IR (ATR): 3429, 3145, 2892, 1722, 1453, 1200, 820, 752, 506 cm^{-1}. ^{1}H NMR (500 MHz, DMSO-d_6) δ 3.45−3.50 (m, 2H, CH_2), 3.53−3.57 (m, 2H, CH_2), 4.36−4.40 (m, 2H, CH_2), 4.47−4.50 (m, 2H, CH_2), 4.70−4.73 (m, 2H, CH_2), 5.63−5.69 (m, 2H, 2CH), 7.12−7.21 (m, 10H, ArH), 8.04 (s, 1H, ArH), 8.09 (s, 1H, ArH). ^{13}C NMR (100 MHz, DMSO-d_6) 37.3 (−ve, CH_2), 63.7 (+ve, CH), 64.1 (−ve, CH_2), 78.4 (+ve, CH), 124.7 (+ve, ArCH), 127.2 (+ve, ArCH), 128.8 (+ve, ArCH), 129.3 (+ve, ArCH), 136.7 (ArC), 143.5 (ArC), 170.2 (C═O), 170.6 (C═O). HRMS (microTOF-QII, MS, ESI): Calcd for $C_{28}H_{28}O_{10}N_6$ ([M − H]$^-$) 607.1783, found 607.1775.

*(S)-2,2′-Bis(prop-2-yn-1-yloxy)-1,1′-binaphthalene (**18**).* Compound **18** was synthesized according to general procedure B using *S*-binol and propargyl bromide. Creamish solid, yield 95%, mp 92 °C. ^{1}H NMR (500 MHz, $CDCl_3$) δ 2.37−2.38 (m, 2H, CH_2), 4.56−4.63 (m, 4H, 2CH_2), 7.12−7.15 (m, 2H, ArH), 7.19−7.22 (m, 2H, ArH), 7.32−7.35 (m, 2H, ArH), 7.56−7.58 (m, 2H, ArH), 7.86−7.88 (d, J = 8.25 Hz, 2H, ArH), 7.96−7.98 (d, J = 8.95 Hz, 2H, ArH). ^{13}C NMR (125 MHz, $CDCl_3$) δ 57.2 (−ve, CH_2), 75.2 (C), 79.3 (+ve, CH), 116.0 (+ve, ArCH), 120.6 (ArC), 124.1 (+ve, ArCH), 125.6 (+ve, ArCH), 126.4 (+ve, ArCH), 127.9 (+ve, ArCH), 129.4 (+ve, ArCH), 129.7 (ArC), 133.9 (ArC), 153.1 (ArC). HRMS (microTOF-QII, MS, ESI): Calcd for $C_{26}H_{18}O_2$ ([M + Na]$^+$) 305.0996, found 305.0984.

*Diethyl 2,2′-((((1,1′-Binaphthalene]-2,2′-diylbis(oxy))bis-(methylene))bis(1H-1,2,3-triazole-5,1-diyl))(S)-diacetate (**19**).* Compound **19** was synthesized according to general procedure E using compound **18** and ethylbromoacetate azide. It was purified by column chromatography with ethyl acetate−hexane (1:1). Creamish solid, yield 87%, mp 96 °C. IR (ATR): 3145, 3056, 2981, 1744, 1595, 1371, 1207, 805, 581 cm^{-1}. ^{1}H NMR (400 MHz, $CDCl_3$) δ 1.24 (t, J = 7.3 Hz, 6H, CH_3), 4.19 (q, J = 7.0 Hz, 4H, 2CH_2), 4.88 (s, 4H, 2CH_2), 5.12 (m, 2H, CH_2), 5.25 (m, 2H, CH_2), 6.79 (s, 2H, ArH), 7.13 (d, J = 8.2 Hz, 2H, ArH), 7.19−7.24 (m, 2H, ArH), 7.32−7.36 (m, 2H, ArH), 7.51 (d, J = 9.1 Hz, 2H, ArH), 7.87 (d, J = 8.2 Hz, 2H, ArH), 7.94 (d, J = 8.7 Hz, 2H, ArH). ^{13}C NMR (100 MHz, $CDCl_3$) δ 14.1 (+ve, CH_3), 50.7 (−ve, CH_2), 62.4 (−ve, CH_2), 63.7 (−ve, CH_2), 115.9 (+ve, ArCH), 120.6 (ArC), 124.0 (+ve, ArCH), 124.1 (+ve, ArCH), 125.5 (+ve, ArCH), 126.5 (+ve, ArCH), 128.0 (+ve, ArCH), 129.5 (+ve, ArCH), 134.0 (ArC), 145.0 (ArC), 153.6 (ArC), 166.25 (C═O). HRMS (microTOF-QII, MS, ESI): Calcd for $C_{34}H_{32}O_6N_6$ ([M + Na]$^+$) 643.2276, found 643.2276.

*Dimethyl 2,2′-(((((S)-[1,1′-Binaphthalene]-2,2′-diyl)bis(oxy))bis-(methylene))bis(1H-1,2,3-triazole-5,1-diyl))(2S,2′S)-bis(3-hydroxypropanoate) (**20**).* Compound **20** was synthesized according to general procedure E using compound **18** and (*S*)-serine methylester azide. Crude product was purified by column chromatography with ethyl acetate−hexane (6:4). Creamish solid, yield 83%, mp 97 °C. IR (ATR): 3280, 3153, 2952, 2117, 1900, 1744, 1595, 1505, 1431, 1326, 1215, 1043, 805, 745, 544 cm^{-1}. ^{1}H NMR (500 MHz, $CDCl_3$) δ 3.70 (s, 3H, OCH_3), 3.73 (s, 3H, OCH_3), 4.11−4.12 (m, 2H, CH_2), 4.21 (m, 1H, CH of CH_2), 4.31−4.32 (m, 1H, CH of CH_2), 4.83−4.92 (m, 2H, CH_2), 5.03−5.05 (m, 1H, CH), 5.10−5.16 (m, 2H, 2CH), 5.28−5.31 (m, 1H, CH), 6.96−7.05 (m, 2H, ArH), 7.13−7.18 (m, 2H, ArH), 7.23−7.24 (m, 2H, ArH), 7.34−7.35 (m, 2H, ArH), 7.48−7.51 (m, 1H, ArH), 7.54−7.59 (m, 1H, ArH), 7.88−7.89 (m, 2H, ArH), 7.93−7.99 (m, 2H, ArH). ^{13}C NMR (125 MHz, $CDCl_3$) δ 53.1 (+ve, OCH_3), 62.8 (−ve, CH_2), 62.9 (−ve, CH_2), 64.7 (+ve, CH), 115.9 (+ve, ArCH), 120.5 (ArC), 124.1 (+ve, ArCH), 124.2 (+ve, ArCH), 125.5 (+ve, ArCH), 126.3 (+ve, ArCH), 128.0 (+ve, ArCH), 129.6 (+ve, ArCH), 129.7 (ArC), 134.0 (ArC), 153.7 (ArC), 167.2 (C═O). HRMS (microTOF-QII, MS, ESI): Calcd for $C_{34}H_{32}O_8N_6$ ([M + Na]$^+$) 675.2174, found 675.2179.

*Dimethyl 2,2′-(((((S)-[1,1′-Binaphthalene]-2,2′-diyl)bis(oxy))bis-(methylene))bis(1H-1,2,3-triazole-5,1-diyl))(2S,2′S)-bis(3-(4-hydroxyphenyl)propanoate) (**21**).* Compound **21** was synthesized according to general procedure E using compound **18** and (*S*)-tyrosine methylester azide and purified by column chromatography with ethyl acetate−hexane (7:3). Creamish solid, yield 86%, mp 86 °C. IR (ATR): 3145, 2952, 2370, 2117, 1893, 1744, 1617, 1513, 1438, 1326, 1207, 1043, 805, 693, 544 cm^{-1}. ^{1}H NMR (500 MHz, DMSO-d_6) δ 3.09−3.14 (m, 2H, CH_2), 3.32−3.35 (m, 2H, CH_2), 3.62 (s, 6H, OCH_3), 5.08−5.16 (m, 4H, 2CH_2), 5.60−5.63 (m, 2H, 2CH), 6.48 (d, J = 8.25 Hz, 4H, ArH), 6.72 (d, J = 8.28 Hz, 4H, ArH), 6.92 (d, J = 8.49 Hz, 2H, ArH), 7.19 (t, J = 7.56 Hz, 2H, ArH), 7.35 (t, J = 7.22 Hz, 2H, ArH), 7.60 (s, 2H, ArH), 7.66 (d, J = 9.02 Hz, 2H, ArH), 7.96 (d, J = 8.17 Hz, 2H, ArH), 8.05 (d, J = 9.21 Hz, 2H, ArH), 9.24 (s, 2H, OH). ^{13}C NMR (125 MHz, DMSO-d_6) δ 36.5 (−ve, CH_2), 53.2 (+ve, OCH_3), 62.8 (−ve, CH_2), 63.8 (+ve, CH), 115.5 (+ve, ArCH), 116.3 (+ve, ArCH), 119.7 (ArC), 124.1 (+ve, ArCH), 124.2 (+ve, ArCH), 125.2 (+ve, ArCH), 125.8 (ArC), 126.8 (+ve, ArCH), 128.4 (+ve, ArCH), 129.4 (ArC), 129.7 (+ve, ArCH), 130.2 (+ve, ArCH), 133.7 (ArC), 143.6 (ArC), 153.9 (ArC), 156.6

https://doi.org/10.1021/acs.jmedchem.1c00880
J. Med. Chem. 2021, 64, 9550−9566

(ArC), 169.0 (C═O). HRMS (microTOF-QII, MS, ESI): Calcd for $C_{46}H_{40}O_8N_6$ ([M + Na]$^+$) 827.2800, found 827.2817.

*Dimethyl 2,2′-(((((S)-[1,1′-Binaphthalene]-2,2′-diyl)bis(oxy))bis-(methylene))bis(1H-1,2,3-triazole-5,1-diyl))(2S,2′S)-bis(3-phenyl-propanoate) (**22**).* Compound **22** was synthesized according to general procedure E using compound **18** and (*S*)-phenylalanine methylester azide. Compound was purified by column chromatography using ethyl acetate−hexane (4:6) as eluent. Creamish solid, yield 84%, mp 89−92 °C. IR (ATR): 3145, 3034, 2952, 2340, 2109, 1893, 1744, 1595, 1431, 1326, 1207, 1043, 909, 805, 574 cm^{-1}. ^{1}H NMR (400 MHz, $CDCl_3$) δ 3.00−3.17 (m, 2H, CH_2), 3.29−3.34 (m, 2H, CH_2), 3.64−3.67 (m, 6H, 2OCH_3), 5.12−5.22 (m, 4H, 2CH_2), 5.24−5.30 (m, 1H, CH), 5.32−5.38 (m, 1H, CH), 6.72−6.73 (m, 1H, ArH), 6.76−6.83 (m, 5H, ArH), 7.03−7.13 (m, 6H, ArH), 7.14−7.18 (m, 2H, ArH), 7.21−7.24 (m, 2H, ArH), 7.34−7.39 (m, 2H, ArH), 7.46 (t, J = 3.6 Hz,1H, ArH), 7.48 (t, J = 3.5 Hz, 1H, ArH), 4.90−4.99 (m, 4H, ArH). ^{13}C NMR (100 MHz, $CDCl_3$) δ 38.3 (−ve, CH_2), 52.9 (+ve, OCH_3), 63.6 (−ve, CH_2), 64.0 (+ve, CH), 115.4 (+ve, ArCH), 120.2 (ArC), 122.4 (+ve, ArCH), 123.9 (+ve, ArCH), 124.0 (+ve, ArCH),125.5 (+ve, ArCH), 126.5 (+ve, ArCH), 127.4 (+ve, ArCH), 128.0 (+ve, ArCH), 128.6 (+ve, ArCH), 129.5 (+ve, ArCH), 133.9 (ArC), 134.6 (ArC), 144.7 (ArC), 144.9 (ArC), 153.4 (ArC), 168.3 (C═O). HRMS (microTOF-QII, MS, ESI): Calcd for $C_{46}H_{40}O_6N_6$ ([M + Na]$^+$) 795.2902, found 795.2899.

*Dimethyl 2,2′-(((((S)-[1,1′-Binaphthalene]-2,2′-diyl)bis(oxy))bis-(methylene))bis(1H-1,2,3-triazole-5,1-diyl))(2S,2′S)-bis(3-(1H-indol-3-yl)propanoate) (**23**).* Compound **23** was synthesized according to the general procedure E using compound **18** and (*S*)-tryptophan methylester azide and purified by column chromatography using ethyl acetate−hexane (6:4) as eluent. Creamish solid, yield 86%, mp 98 °C. IR (ATR): 3406, 3056, 2117, 1997, 1893, 1744, 1587, 1431, 1334, 1207, 1043, 805, 745, 581 cm^{-1}. ^{1}H NMR (500 MHz, $CDCl_3$) δ 3.02−3.14 (m, 2H, CH_2), 3.29−3.36 (m, 2H, CH_2), 3.64−3.67 (m, 6H, 2OCH_3), 5.11−5.21 (m, 4H, 2CH_2), 5.25−5.28 (m, 1H, CH), 5.29−5.37 (m, 1H, CH), 6.72−6.74 (m, 1H, ArH), 6.77−6.81 (m, 3H, ArH), 7.04−7.11 (m, 6H, ArH), 7.13−7.18 (m, 2H, ArH), 7.21−7.23 (m, 2H, ArH), 7.34−7.38 (m, 2H, ArH), 7.46−7.49 (m, 2H, ArH), 7.89−7.91 (m, 2H, ArH), 7.94−7.98 (m, 2H, ArH). ^{13}C NMR (100 MHz, $CDCl_3$) δ 28.6 (−ve, CH_2), 53.0 (+ve, OCH_3), 63.1 (+ve, CH), 63.1 (−ve, CH_2), 107.7 (ArC), 111.6 (+ve, ArCH), 116.1 (+ve, ArCH), 117.5 (+ve, ArCH), 119.5 (+ve, ArCH), 120.5 (ArC), 122.0 (+ve, ArCH), 123.1 (+ve, ArCH), 124.1 (+ve, ArCH), 125.3 (+ve, ArCH), 126.3 (ArC), 126.4 (+ve, ArCH), 127.8 (+ve, ArCH), 129.2 (+ve, ArCH), 129.3 (ArC), 133.8 (ArC), 135.7 (ArC), 144.1 (ArC), 153.4 (ArC), 168.7 (C═O). HRMS (microTOF-QII, MS, ESI): Calcd for $C_{50}H_{42}O_6N_8$ ([M + Na]$^+$) 873.3120, found 873.3092.

Lipoxygenase Inhibitory Activities. For LOX inhibition studies, solutions of compounds at 10^{-4}, 10^{-5}, 10^{-6}, 10^{-7}, and 10^{-8} concentrations were prepared in DMSO. Ten microliters of each compound from the above concentrations was added to 90 μL of LOX (Soyabean lipoxygenase) solution in assay buffer taken in the wells of a 96-well plate. Each compound was tested in triplicate, and the average of three values with deviation <5% was taken for calculation. Two wells were taken as blanks (assay buffer + AA), and four wells were taken as positive controls (enzyme in assay buffer + AA). The reaction was initiated by the addition of 10 μL of the substrate (AA). After shaking the 96-well plate on a shaker for 5 min, 100 μL of the chromogen (developing reagent) was added to each well. The plate was again shaken for 5 min and read at 490 nm in a microplate scanning spectrophotometer. Percent LOX inhibitory activity was determined using the average of the two values for each sample

$$[\text{A500/min} / 9.47\ \text{mM}^{-1}] \times [0.21\ \text{mL}/0.09\ \text{mL}] \times \text{sample dilution}$$

where:

A500/min = A500 (sample)/min − A500 (blank)/5 min,

9.47 mM^{-1} = extinction coefficient of chromogen,

0.21 mL = total volume of the solution in each well, and

0.09 mL = volume of the enzyme solution used.

Percent LOX inhibition = [{L.A. (P.C.) − L.A. (I.)}/L.A. (P.C.)] × 100.

L.A. (P.C.) = lipoxygenase activity of positive control, L.A. (I.) = lipoxygenase activity of inhibitor. IC_{50} values were determined from the graph between percent inhibition versus concentration of inhibitor.

COX-1 and COX-2 Inhibitory Immunoassay. The inhibitory activities of all the synthesized compounds against COX-1 (ovine) and COX-2 (human) were determined. Five different concentrations (10^{-4} to 10^{-8} M) of the compounds were prepared, and their enzyme-inhibition assay was performed in triplicate as per the protocol available with the COX Inhibitory Screening Assay Kit. The background samples of both COX-1 and COX-2 were prepared by putting 20 μL of each enzyme into separate test tubes and keeping them in boiling water for 3 min. The background tubes for COX-1 and COX-2 were prepared by adding 160 μL of reaction buffer, 10 μL of heme, and 10 μL of inactive COX-1 or COX-2. The initial activity tubes of COX-1 and COX-2 were prepared by adding 160 μL of reaction buffer, 10 μL of heme, and 10 μL of COX-1 and COX-2 enzyme to the respective tubes. The COX-1 and COX-2 inhibitor tubes were prepared by adding 160 μL of reaction buffer, 10 μL of heme, 10 μL of COX-1 or COX-2, and 10 μL of inhibitor solution. After the incubation of the tubes at 37 °C for 10 min, 10 μL of arachidonic acid was added to each of the tubes, which were incubated at 37 °C for 2 min. The reaction was quenched by adding 30 μL of saturated $SnCl_2$ to each reaction tube. As described in a previous report,[61] the prostaglandins produced in each well were quantified using EIA.

Human Whole Blood Assay. The protocol for human whole blood assay was approved by the Institutional Ethics Committee of Guru Nanak Dev University, Amritsar, and the assay was performed as per the procedure described in the previous report.[61]

Carrageenan Induced-Paw Edema Test. Swiss albino mice of either sex weighing 25−35 g were used for the present studies. The animals were kept under 12 h light/12 h dark cycle with free supply of food and water and maintaining the temperature at 22 ± 2 °C. All the protocols for animal studies were approved by the Institutional Animal Ethical Committee (IAEC) of Guru Nanak Dev University, Amritsar, Punjab, India. The animals were divided into different groups of six animals in each group. Group I, the control, comprised of animals treated with vehicle (acetic acid/carrageenan), and group II was treated with the standard reference drug indomethacin (10 mg kg^{-1}). The other group/s of animals was/were administered test compounds at doses of 5 mg kg^{-1} and variable doses in the case of compound **15** (for dose−response assay).

100 μL of freshly prepared 1% carrageenan solution was injected on the subplantar surface of the hind paw to induce paw edema. Thirty min before carrageenan injection, standard and treatment groups received indomethacin (10 mg kg^{-1}) and test compounds (5 mg kg^{-1}), respectively. Paw thickness (mm) was determined at different time intervals after carrageenan administration (15, 30, 60, 120, 180, 240, 300, and 360 min). A decrease in paw thickness (mm) was taken as a measure of the anti-inflammatory potential of the standard and the test compounds.

Acetic Acid-Induced Writhing Test. Acetic acid-induced writhing is a screening model for assessing analgesic agents. Writhings were indicated by stretching of the abdomen and extension of hind-limbs. Writhings were induced by injecting freshly prepared 0.6% v/v acetic acid solution intraperitonealy 30 min before acetic acid injection; standard and treatment groups (six animals in each group) received indomethacin (10 mg kg^{-1}) and test compounds (5 mg kg^{-1}), respectively. Thereafter, mice were placed in a transparent box and the number of abdominal writhings was noted for 30 min.

Acute Toxicity Study. Acute toxicity studies were carried out using Swiss albino mice. Briefly, 2 groups were used with three animals in each group (n = 3). The first group was taken as normal control while in the second group of animals, compound **15** was given orally at a dose of 300 mg kg^{-1}. The study was performed after 4 h of

https://doi.org/10.1021/acs.jmedchem.1c00880
J. Med. Chem. 2021, 64, 9550−9566

the fasting period. Mice were continuously monitored for a period of 4 h followed by periodic monitoring for the next 14 days.

Mechanistic Study. Three animal groups (n = 6) were utilized to study the involvement of cyclooxygenase, lipoxygenase, and the nitric oxide pathway in modulating the analgesic potential of the most active compound. Substance-P (10 μg kg^{-1}) was utilized to study the involvement of COX-2 and LOX pathways. The nitric oxide donor L-arginine (40 mg kg^{-1}) and nitric oxide synthase inhibitor N6-(1-Iminoethyl)-L-lysine-dihydrochloride (L-NIL) (5 mg kg^{-1}) were utilized to study the involvement of nitric oxide. Thirty minutes before treatment with the test compound, the three groups of animals received substance-P, L-arginine, and L-NIL, respectively. After 30 min, each group was treated with 0.6% v/v acetic-acid, and the number of abdominal writhings was noted for 30 min.

In Vivo Pharmacokinetic Studies. The in vivo PK studies were evaluated using Swiss Albino mice (25−35 g) of either sex (10 groups with three animals in each group). Ten mg kg^{-1} dose of compound **15** was suspended in 0.1% CMC and administered intraperitonealy. The animals were anesthetized with ketamine (50 mg kg^{-1} i.p.). The blood samples were withdrawn from the jugular vein at intervals of 30, 45, and 60 min and 2, 3, 4, 6, 8, 11, and 24 h and collected in heparinised tubes. Samples were withdrawn in triplicate (3 samples/time interval). 100 μL of blood sample was withdrawn at each interval from one animal. Further, the samples were prepared for LC-MS studies using the procedure as described in the previous report.[62]

Molecular Docking Studies. The molecular docking of the compounds was performed in the active site pockets of COX-2 (pdb ID 1CVU)[63] and 5-LOX (pdb ID 3V99)[64] using the procedure as described in one of the previous reports.[61]

ADME properties were calculated using online PreADMET software.[53]

Isothermal Titration Calorimetry Experiments. For ITC experiments, solutions of compound **15** (100 μM) were prepared in HPLC grade DMSO and 0.1 M Tris-Buffer (1:9) and enzyme (COX-1, COX-2, 5-LOX) by dissolving 10 μL in 5 mL of Tris-buffer, and solutions of HSA were prepared by dissolving 0.05 g of HSA in 1 mL of Tris-Buffer. Enzyme solution in Tris-buffer was taken into the sample cell and was titrated against the compound taken in a rotating stirrer syringe (500 rpm) at 25 °C. Each experiment consists of 40 consecutive injections of 1 μL of the compound into the enzyme solution, except in the case of COX-1, for which 20 injections were there each of 2 μL, after regular time intervals of 120 s so that equilibrium was attained at each titration point. The total heat, Q, produced or absorbed by the active cell was determined at fractional saturation Θ after the ith injection given by the equation

$$Q = n\Theta \mathrm{Mt}\Delta H V_o$$

where Mt is the total concentration of the enzyme, V_o is the cell volume, n is the total number of binding sites in the enzyme, and ΔH is the molar heat of ligand binding. The enthalpy change for the ith injection, $\Delta H(i)$, for an injection volume dVi is defined by the equation

$$\Delta H(i) = Q(i) + \mathrm{d}Vi/V_o[Q(i) - Q(i-1)/2] - Q(i-1)$$

The control titrations consisting of identical titrant solution with the same cell filled just with the buffer solution and also the successive buffer additions to the enzyme solution were carried out to determine the background heat which was to be subtracted from the main experiment. This was done to eliminate the heat of mixing and the heat of dilution. Origin 7.0 software by Microcal was used to read the titration-heat profiles for calculating the binding parameters. The single-binding-site model was used to fit the data, and the K_a and binding enthalpy (ΔH), Gibbs free energy (ΔG), and entropy (ΔS) were calculated.

■ ASSOCIATED CONTENT

Supporting Information

The Supporting Information is available free of charge at https://pubs.acs.org/doi/10.1021/acs.jmedchem.1c00880.

^{1}H and ^{13}C NMR spectra, mass spectra, and molecular docking data (PDF)

Homology Models: NA Molecular formula strings of compounds **6**−**23** (CSV)

PDB coordinates for computational models. Three-dimensional models of target−ligand (compounds docked in COX-2, 5-LOX) complexes (ZIP)

■ AUTHOR INFORMATION

Corresponding Author

Palwinder Singh − *Department of Chemistry, Guru Nanak Dev University, Amritsar 143005, India;* orcid.org/0000-0003-2332-5257; Email: palwinder_singh_2000@yahoo.com

Authors

Priya Kumari − *Department of Chemistry, Guru Nanak Dev University, Amritsar 143005, India;* orcid.org/0000-0002-1802-5412

Jashanpreet Kaur − *Department of Pharmaceutical Sciences, Guru Nanak Dev University, Amritsar 143005, India*

Rajbir Bhatti − *Department of Pharmaceutical Sciences, Guru Nanak Dev University, Amritsar 143005, India;* orcid.org/0000-0002-5761-7074

Complete contact information is available at: https://pubs.acs.org/10.1021/acs.jmedchem.1c00880

Notes

The authors declare no competing financial interest.

■ ACKNOWLEDGMENTS

Financial assistance from CSIR, New Delhi, is gratefully acknowledged. P.K. thanks SERB-DST, New Delhi, for JRF.

■ ABBREVIATIONS USED

AA, arachidonic acid; COX-2, cyclooxygenase-2; COX-1, cyclooxygenase-1; IC_{50}, 50% inhibitory concentration; IL-6, interleukin; i.p., intraperitoneally; L-NIL, N6-(1-iminoethyl)-L-lysine-dihydrochloride; LOX, lipoxygenase; LPS, lipopolysaccharide; LT4, leukotriene; NaH, sodium hydride; SEM, standard error mean; THF, tetrahydrofuran

■ REFERENCES

(1) Ward, P. A. Acute and chronic inflammation. In *Fundamentals of inflammation*; Serhan, C. N., Ward, P. A., Gilroy, D. W., Eds.; Cambridge University Press: Cambridge, 2010; pp 1−16.

(2) Ridker, P. M.; Cushman, M.; Stampfer, M. J.; Tracy, R. P.; Hennekens, C. H. Inflammation, aspirin and the risk of cardiovascular disease in apparently healthy man. *N. Engl. J. Med.* **1997**, *336*, 973−979.

(3) Marnett, L. J. Inflammation and cancer: Chemical approaches to mechanisms, imaging, and treatment. *J. Org. Chem.* **2012**, *77*, 5224−5238.

(4) Stevens, R. J.; Douglas, M. J. K.; Saratzis, A. N.; Kitas, G. D. Inflammation and atherosclerosis in rheumatoid arthritis. *Expert Rev. Mol. Med.* **2005**, *7*, 1−24.

(5) Donath, M. Y.; Shoelson, S. E. Type 2 diabetes as an inflammatory diseases. *Nat. Rev. Immunol.* **2011**, *11*, 98−107.

(6) Hoozemans, J. J. M.; O'Banion, M. K. The role of COX-1 and COX-2 in Alzheimer's disease pathology and the therapeutic potential of non-steroidal anti-inflammatory drugs. *Curr. Drug Targets: CNS Neurol. Disord.* **2005**, *4*, 307−315.

(7) Yokoyama, C.; Tanabe, T. Cloning of human gene encoding prostaglandin endoperoxide synthase & primary structure of enzyme. *Biochem. Biophys. Res. Commun.* **1989**, *165*, 888−894.
(8) Feng, L.; Sun, W.; Xia, Y.; Tang, W. W.; Chanmugam, P.; Soyoola, E.; Wilson, C. B.; Hwang, B. Cloning of two isoforms of rat cyclooxygenase: Differential regulation of their expression. *Arch. Biochem. Biophys.* **1993**, *307*, 361−368.
(9) Hla, T.; Neilson, K. Human cyclooxygenase-2. *Proc. Natl. Acad. Sci. U. S. A.* **1992**, *89*, 7384−7388.
(10) Jones, D. A.; Carlton, D. P.; McIntyre, T. M.; Zimmermans, G. A.; Prescott, S. M. cDNA Molecular cloning of human prostaglandin endoperoxide synthase type II and demonstration of expression in response to cytokines. *J. Biol. Chem.* **1993**, *268*, 9049−9054.
(11) Proschak, E.; Heitel, P.; Kalinowsky, L.; Merk, D. Opportunities and challenges for fatty acid mimetics in drug discovery. *J. Med. Chem.* **2017**, *60*, 5235−5266.
(12) Martel-Pelletier, J.; Lajeunesse, D.; Reboul, P.; Pelletier, J. Therapeutic role of dual inhibitors of 5-LOX and COX, selective and non-selective non-steroidal anti-inflammatory drugs. *Ann. Rheum. Dis.* **2003**, *62*, 501−509.
(13) Haeggstrom, J. Z.; Funk, C. D. Lipoxygenase and leukotriene pathways: Biochemistry, biology, and roles in disease. *Chem. Rev.* **2011**, *111*, 5866−5898.
(14) Nakamura, M.; Shimizu, T. Leukotriene Receptors. *Chem. Rev.* **2011**, *111*, 6231−6298.
(15) Funk, C. D. Prostaglandins and leukotrienes: Advances in Eicosanoid Biology. *Science* **2001**, *294*, 1871−1875.
(16) Lai, S. T. Treatment of severe acute respiratory syndrome. *Eur. J. Clin. Microbiol. Infect. Dis.* **2005**, *24*, 583−591.
(17) Zidar, N.; Odar, K.; Glavac, D.; Jerse, M.; Zupanc, T.; Stajer, D. Cyclooxygenase in normal human tissues- Is COX-1 really a constitutive isoform and COX-2 an inducible form. *J. Cell Mol. Med.* **2009**, *13*, 3753−3763.
(18) Flower, R. J. The development of cox-2 inhibitors. *Nat. Rev. Drug Discovery* **2003**, *2*, 179−191.
(19) Prasit, P.; Wang, Z.; Brideau, C.; Chan, C.-C.; Charleson, S.; Cromlish, W.; Ethier, D.; Evans, J. F.; Ford- Hutchinson, A. W.; Gauthier, J. Y.; Gordon, R.; Guay, J.; Gresser, M.; Kargman, S.; Kennedy, B.; Leblanc, Y.; Leger, S.; Mancini, J.; Oneill, G. P.; Ouellet, M.; Percival, M. D.; Perrier, H.; Riendeau, D.; Rodger, I.; Tagari, P.; Therien, M.; Vickers, P.; Wong, E.; Xu, L.-J.; Young, R. N.; Zamboni, R. The discovery of Rofecoxib, [MK 966, VIOXX, 4-(4′-\ methylsuphonylphenyl)-3-phenyl-2(5H)-furanone], an orally active cyclooxygenase-2 inhibitor. *Bioorg. Med. Chem. Lett.* **1999**, *9*, 1773−1778.
(20) Singh, P.; Mittal, A. Current status of COX-2 inhibitors. *Mini-Rev. Med. Chem.* **2008**, *8*, 73−90.
(21) Mohsin, N.-U.-A.; Irfan, M. Selective cyclooxygenase-2 inhibitors: A review of recent chemical scaffolds with promising anti-inflammatory and COX-2 inhibitory activities. *Med. Chem. Res.* **2020**, *29*, 809−830.
(22) Cotter, J.; Wooltorton, E. New restrictions on celecoxib (Celebrex) use and the withdrawal of valdecoxib (Bextra). *Can. Med. Assoc. J.* **2005**, *172*, 1299.
(23) *Merck announces voluntary worldwide withdrawal of VIOXX®. News release*; Merck: Whitehouse Station, NJ, 2004. www.vioxx.com/vioxx/documents/english/vioxx_press_release.pdf.
(24) Penning, T. D.; Tally, J. J.; Bertenshaw, S. R.; Carter, J. S.; Collins, P. W.; Docter, S.; Graneto, M. J.; Lee, L. F.; Malecha, J. W.; Miyashiro, J. M.; Rogers, R. S.; Koboldt, C. M.; Perkins, W. E.; Seibert, K.; Veenhuizen, A. W.; Zhang, Y. Y.; Isakson, P. C. Synthesis and biological evaluation of the 1,5-diarylpyrazole class of cyclooxygenase-2 inhibitors: Identification of 4-[5-(4-methylphenyl)-3-(trifluoromethyl)-1*H*-pyrazol-1-yl]benzenesulfonamide (SC-58635, Celecoxib). *J. Med. Chem.* **1997**, *40*, 1347−1365.
(25) Chan, F. K. L.; Hung, L. C. T.; Suen, B. Y.; Wu, J. C. Y.; Lee, K. C.; Leung, V. K. S.; Hui, A. J.; To, K. F.; Leung, W. K.; Wong, V. W. S.; Chung, S. C. S.; Sung, J. J. Y. Celecoxib versus diclofenac and omeprazole in reducing the risk of recurrent ulcer bleeding in patients with arthritis. *N. Engl. J. Med.* **2002**, *347*, 2104−2110.
(26) Proschak, E.; Heitel, P.; Kalinowsky, L.; Merk, D. Opportunities and challenges for fatty acid mimetics in drug discovery. *J. Med. Chem.* **2017**, *60*, 5235−5266.
(27) Yang, K.; Ma, W.; Liang, H.; Ouyang, Q.; Tang, C.; Lai, L. Dynamic simulations on the arachidonic acid metabolic network. *PLoS Comput. Biol.* **2007**, *3*, 0523−0530.
(28) Charlier, C.; Michaux, C. Dual inhibition of cyclooxygenase-2 (COX-2) and 5-lipoxygenase (5-LOX) as a new strategy to provide safer non-steroidal anti-inflammatory drugs. *Eur. J. Med. Chem.* **2003**, *38*, 645−659.
(29) Jacob, P. J.; Manju, S. L.; Ethiraj, K. R.; Elias, G. Safer anti-inflammatory therapy through dual COX-2/5-LOX inhibitors: A structure-based approach. *Eur. J. Pharm. Sci.* **2018**, *121*, 356−381.
(30) Carter, G. W.; Young, P. R.; Albert, D. H.; Bouska, J.; Dyer, R.; Bell, R. L.; Summers, J. B.; Brooks, D. W. 5-Lipoxygenase inhibitory activity of zileuton. *J. Pharmacol. Exp. Ther.* **1991**, *256*, 929−937.
(31) Dogne, J.-M.; Supuran, C. T.; Pratico, D. Adverse cardiovascular effects of the coxibs. *J. Med. Chem.* **2005**, *48*, 2251−2256.
(32) White, W. B.; West, C. R.; Borer, J. S.; Gorelick, P. B.; Lavange, L.; Pan, S. X.; Weiner, E.; Verburg, K. M. Risk of cardiovascular events in patients receiving celecoxib: A meta-analysis of randomized clinical trials. *Am. J. Cardiol.* **2007**, *99*, 91−98.
(33) Solomon, S. D.; McMurray, J. J. V.; Pfeffer, M. A.; Wittes, J.; Fowler, R.; Finn, P.; Anderson, W. F.; Zauber, A.; Hawk, E.; Bertagnolli, M. Cardiovascular risk associated with celecoxib in a clinical trial for colorectal adenoma prevention. *N. Engl. J. Med.* **2005**, *352*, 1071−1080.
(34) Berger, W.; De Chandt, M. T. M.; Cairns, C. B. Zileuton: clinical implications of 5-lipoxygenase inhibition in severe airway disease. *Int. J. Clin. Pract.* **2007**, *61*, 663−676.
(35) Larsson, B.-M.; Kumlin, M.; Sundblad, B.-M.; Larsson, K.; Dahlon, S.-E; Palmberg, L. Effects of 5-lipoxygenase inhibitor zileuton on airway responses to inhaled sewine house dust in healthy subject. *Respir. Med.* **2006**, *100*, 226−237.
(36) Singh, P.; Kaur, J.; Singh, G.; Bhatti, R. Triblock conjugates: Identification of a highly potent antiinflammatory agent. *J. Med. Chem.* **2015**, *58*, 5989−6001.
(37) Singh, P.; Prasher, P.; Dhillon, P.; Bhatti, R. Indole based peptidomimetics as anti-inflammatory and antihyperalgesic agents: Dual inhibition of 5-LOX and COX-2 enzymes. *Eur. J. Med. Chem.* **2015**, *97*, 104−123.
(38) Gouda, A. M.; Ali, H. I.; Almalki, W. H.; Azim, M. A.; Abourehab, M. A. S.; Abdelazeem, A. H. Design, synthesis, and biological evaluation of some novel pyrrolizine derivatives as COX inhibitors with anti-inflammatory/analgesic activities and low ulcerogenic liability. *Molecules* **2016**, *21* (2), 201.
(39) Shen, F.-Q.; Wang, Z.-C.; Wu, S.-Y.; Ren, S.-Z.; Man, R.-J.; Wang, B.-Z.; Zhu, H.-L. Synthesis of novel hybrids of pyrazole and coumarin as dual inhibitors of COX-2 and 5-LOX. *Bioorg. Med. Chem. Lett.* **2017**, *27*, 3653−3660.
(40) Chowdhury, M. A.; Abdellatif, K. R. A; Dong, Y.; Das, D.; Suresh, M. R.; Knaus, E. E. Synthesis of celecoxib analogues possessing a N-difluoromethyl-1,2-dihydropyrid-2-one 5-lipoxygenase pharmacophore: Biological evaluation as dual inhibitors of cyclooxygenases and 5-lipoxygenase with anti-inflammatory activity. *J. Med. Chem.* **2009**, *52*, 1525−1529.
(41) Elkady, M.; Nieß, R.; Schaible, A. M.; Bauer, J.; Luderer, S.; Ambrosi, G.; Werz, O.; Laufer, S. A. Modified acidic nonsteroidal anti-inflammatory drugs as dual inhibitors of mPGES-1 and 5-LOX. *J. Med. Chem.* **2012**, *55*, 8958−8962.
(42) Pommery, N.; Taverne, T.; Telliez, A.; Goossens, L.; Charlier, C.; Pommery, J.; Goossens, J.-F.; Houssin, R.; Durant, F.; Hénichart, J.-P. New COX-2/5-LOX Inhibitors: Apoptosis-inducing agents potentially useful in prostate cancer chemotherapy. *J. Med. Chem.* **2004**, *47*, 6195−6206.

https://doi.org/10.1021/acs.jmedchem.1c00880
J. Med. Chem. 2021, 64, 9550−9566

(43) Sharma, V.; Bhatia, P.; Alam, O.; Naim, M. J.; Nawaz, F.; Sheikh, A. A.; Jha, M. Recent advancement in the discovery and development of COX-2 inhibitors: Insight into biological activities and SAR studies (2008−2019). *Bioorg. Chem.* **2019**, *89* (1−45), 103007.
(44) Dheer, D.; Singh, V.; Shankar, R. Medicinal attributes of 1,2,3-triazoles: Current developments. *Bioorg. Chem.* **2017**, *71*, 30−54.
(45) Kharb, R.; Sharma, R. C.; Yar, M. S. Pharmacological significance of triazole scaffold. *J. Enzyme Inhib. Med. Chem.* **2011**, *26*, 1−21 and references therein.
(46) *COX Inhibitory Screening Assay Kit (no. 560131)*; Cayman Chemicals.
(47) *5-LOX inhibitor screening assay kit, Item No. 760700*; Cayman Chemical Co.
(48) *TXB_2 Express ELISA kit-monoclonal, item No. 10004023*; Cayman Chemical Co.
(49) Tadiwos, Y.; Nedi, T.; Engidawork, E. Analgesic and anti-inflammatory activities of 80% methanol root extract of Jasminumabys-sinicumhochst. ex. Dc. (Oleaceae) in mice. *J. Ethnopharmacol.* **2017**, *202*, 281−289.
(50) Singh, P.; Kaur, S.; Kumari, P.; Kaur, B.; Kaur, M.; Singh, G.; Bhatti, R.; Bhatti, M. Tailoring the substitution pattern on 1,3,5-triazine for targeting cyclooxygenase-2: Discovery and structure-activity relationship of triazine-4-aminophenylmorpholin-3-one hybrids that reverse algesia and inflammation in Swiss Albino mice. *J. Med. Chem.* **2018**, *61*, 7929−7941.
(51) Winter, C. A.; Risely, E. A.; Nuss, G. W. Carrageenan induced edema in hind paw of the rat as an assay for anti-inflammatory drugs. *Exp. Biol. Med.* **1962**, *111*, 544−547.
(52) Guirguis, M. S.; Sattari, S.; Jamali, F. Pharmacokinetics of celecoxib in the presence and absence of interferon-induced acute inflammation in the rat: Application of a novel HPLC assay. *J. Pharm. Pharmaceut. Sci.* **2001**, *4*, 1−6.
(53) *SEOUL, SOUTH KOREA: BIOINFORMATICS AND MOLECULAR DESIGN RESEARCH CENTER*; 2004. PREADMET PROGRAM. Available from URL: http://preadmet.bmdrc.org.
(54) Vecchio, A. J.; Orlando, B. J.; Nandagiri, R.; Malkowski, M. G. Investigating substrate promiscuity in cyclooxygenase-2: The role of Arg-120 and residues lining the hydrophobic groove. *J. Biol. Chem.* **2012**, *287*, 24619−24630.
(55) Bhattacharyya, D. K.; Lecomte, M.; Rieke, C. J.; Garavito, R. M.; Smith, W. L. Involvement of arginine 120, glutamate 524, and tyrosine 355 in the binding of arachidonate and 2-phenylpropionic acid inhibitors to the cyclooxygenase active site of ovine prostaglandin endoperoxide H synthase-1. *J. Biol. Chem.* **2003**, *278*, 45763−45769.
(56) Rieke, C. J.; Mulichak, A. M.; Garavito, R. M.; Smith, W. L. The role of arginine 120 of human prostaglandin endoperoxide H synthase-2 in the interaction with fatty acid substrates and inhibitors. *J. Biol. Chem.* **1999**, *274*, 17109−17114.
(57) Rowlinson, S. W.; Kiefer, J. R.; Prusakiewicz, J. J.; Pawlitz, J. L.; Kozak, K. R.; Kalgutkar, A. S.; Stallings, W. C.; Kurumbail, R. G.; Marnett, L. J. A novel mechanism of cyclooxygenase-2 inhibition involving interactions with Ser-530 and Tyr-385. *J. Biol. Chem.* **2003**, *278*, 45763−45769.
(58) Hochgesang, G. P.; Rowlinson, S. W.; Marnett, L. J. Tyrosine-385 is critical for acetylation of cyclooxygenase-2 by aspirin. *J. Am. Chem. Soc.* **2000**, *122*, 6514−6515.
(59) Shimokawa, T.; Kulmacz, R. J.; DeWitt, D. L.; Smith, W. L. Tyrosine 385 of prostaglandin endoperoxide synthase is required for cyclooxygenase. *J. Biol. Chem.* **1990**, *265*, 20073−20076.
(60) Pauli, G. F.; Chen, S.-N.; Simmler, C.; Lankin, D. C.; Godecke, T.; Jaki, B. U.; Friesen, J. B.; McAlpine, J. B.; Napolitano, J. G. Importance of purity evaluation and the potential of quantitative ^{1}H NMR as a purity assay. *J. Med. Chem.* **2014**, *57*, 9220−9231.
(61) Singh, P.; Kaur, S.; Kaur, J.; Singh, G.; Bhatti, R. Rational design of small peptides for optimal inhibition of cyclooxygenase-2: Development of a highly effective anti-inflammatory agent. *J. Med. Chem.* **2016**, *59*, 3920−3934.
(62) Kaur, S.; Kumar, P.; Singh, G.; Bhatti, R.; Singh, P. Design and synthesis of aza-/oxa-heterocycle-based conjugates as novel anti-inflammatory agents targeting cyclooxygenase-2. *ACS Omega* **2018**, *3*, 5825−5845.
(63) Kiefer, J. R.; Pawlitz, J. L.; Moreland, K. L.; Stegeman, R. A.; Hood, W. F.; Gierse, J. K.; Stevens, A. M.; Goodwin, D. C.; Rowlinson, S. W.; Marnett, L. J.; Stallings, W. C.; Kurumbail, R. G. Structural insights into the stereochemistry of the cyclooxygenase reaction. *Nature* **2000**, *405*, 97−101.
(64) Gilbert, N. C.; Rui, Z.; Neau, D. B.; Waight, M. T.; Bartlett, S. G.; Boeglin, W. E.; Brash, A. R.; Newcomer, M. E. Conversion of human 5-lipoxygenase to a 15-lipoxygenase by a point mutation to mimic phosphorylation at serine-663. *FASEB J.* **2012**, *26*, 3222−3229.

https://doi.org/10.1021/acs.jmedchem.1c00880
J. Med. Chem. 2021, 64, 9550−9566